Neuroscience Applied 5 (2026) 106988

Contents lists available at ScienceDirect

Neuroscience Applied

journal homepage: www.journals.elsevier.com/neuroscience-applied

Review

Differentiation of human iPSCs into dopaminergic neurons: comparative analysis of 2D and 3D protocols for disease modeling and pharmacology

Giulia Sofia Marcotto [a], Jonida Bitraj [a], Emilio Merlo Pich [b], Ginetta Collo [a,*]

[a] Department of Molecular and Translational Medicine, University of Brescia, Brescia, Italy
[b] Gelf Health, Milano, Italy

ARTICLE INFO

Keywords:
Midbrain
Organoids
Drug screening
Personalized medicine
Induced pluripotent stem cells
Parkinson's disease

ABSTRACT

This pragmatic review addresses those protocols containing innovative steps for differentiating human inducible Pluripotent Stem Cells (iPSCs) into mature midbrain dopaminergic (mDA) neurons, leading to successful implementation in other articles of in vitro models for neurodegenerative or psychiatric disorders and for pharmacological tests, in the period 2004-2025. Article were selected according to the presence of protocols that allowed the iPSC differentiation into mDA neurons as defined by the expression of DA neural lineage markers and Thyrosine Hydroxylase, by the evidence of neuronal morphology, electrophysiology, neurochemistry, biomarkers and intracellular depositions that recapitulate various stages of differentiation and maturation of the mammalian brain mDA neuron. The critical innovative aspects that allowed the article selection was the presence of a significative methodological step in increasing the protocol performance and the useful replicability in term the number of peer-reviewed articles implementing this procedure. Out of 108 articles of protocols based on stem cells-derived mDA neurons, we identified 12 articles regarding 2-dimensional (2D) cultures and 11 articles regarding 3-dimensional (3D)/organoid cultures. For 2D cultures, the most effective protocol would include a floor plate induction with dual-SMAD inhibition improved by a biphasic WNT activation process and by a pre-differentiation step of neural precursor expansion. Regarding the more recent protocols for 3D midbrain-like organoids, less disease model articles were generated, requiring more time for assessing of the most performing protocols. 3D/organoids were found superior to 2D cultures since they better represent the original midbrain neuronal circuitry, allowing better personalized disease modelling.

1. Introduction

Several neurodegenerative and psychiatric disorders are associated with dysfunctions of the dopaminergic (DA) system in its various substructures. The nigrostriatal DA pathway is critical for voluntary movement and body posture, and its selective degeneration is a hallmark of Parkinson's Disease (PD) (Bloem et al., 2021), while the mesocortical and mesolimbic DA circuits support cognitive, emotional and reward-related processes, their dysregulation playing a critical role in the pathogenesis of multiple psychiatric conditions, including schizophrenia and mood disorders (Grace, 2016). Most of these DA circuits originate from DA neurons localized in the midbrain (midbrain DA (mDA) neurons). A variety of pathogenic processes converge on these circuits leading to maladaptive responses to cellular stressors such as oxidative, proinflammatory, hypoxic stimuli, as well as exposure to environmental toxicants, viral infections, and by sustained hyperactivity within neuronal networks (e.g., abnormal firing rates). These stressors initially produce molecular changes leading to impaired functionality and neuroplasticity and, when neurodegeneration occurs, to neuronal loss and atrophy (Tesco and Lomoio, 2022). Notably, some constitutive aspects of the mDA neurons, including their phenotype, genetic and epigenetic profile, as well as mitochondrial function, make this cell population particularly susceptible to harmful conditions. mDA neurons are highly sensitive to oxidative stress due to their high rate of oxygen metabolism, low levels of intracellular antioxidants, and elevated iron content (Dong-Chen et al., 2023) that may all conjure to affect mDA neuron development, connectivity, plasticity and synaptic signaling reported in neurological and psychiatric disorders (Grace, 2016; Klein et al., 2019; Xu and Yang, 2022). While the modelling of the general features of various neuronal pathogenic mechanisms have benefited from animal models and immortalized cell cultures, the specific features affecting only certain individuals, and not others, are becoming a

* Corresponding author. Department of Molecular and Translational Medicine, University of Brescia, Viale Europa 11, 25123, Brescia, Italy.
E-mail address: luigia.collo@unibs.it (G. Collo).

https://doi.org/10.1016/j.nsa.2026.106988
Received 22 November 2025; Received in revised form 30 January 2026; Accepted 10 February 2026
Available online 12 February 2026

relevant problem, particularly in the age of 'personalized medicine'. Human-originated tissues became more appreciated in view of their translational relevance. Moreover, modeling sub-groups of affected individuals characterized by common genetic or molecular underpinnings resulted in the successful implementation of precision medicine in oncology, allowing a rational targeting of specific dysfunctional molecular pathways with selective drugs (Wang and Wang, 2023). Applying a similar strategy to brain disorders is challenging because the living brain tissue is rarely accessible and post-mortem samples are heavily influenced by heterogenous clinical profiles, premorbid conditions and handling procedures, which limit data quality and interpretation. To bypass these obstacles, patient-derived stem cell approaches were developed. Early studies showed that human Embryonic Stem Cells (ESC) from the blastocyst inner cell mass can generate multiple neural lineages, including DA neurons (Anselme L. Perrier et al., 2004; Sonntag et al., 2007; Van Inzen et al., 1996), but ethical issues and narrow disease-related conditions restricted their applicability. A major advance came with induced Pluripotent Stem Cells (iPSCs), introduced in 2006–2007 (Takahashi et al., 2007; Takahashi and Yamanaka, 2006), whose innovative value was recognized with the Nobel Prize awarded to Shinya Yamanaka in 2012. Presently, the use of human iPSCs in personalized medicine is rapidly expanding because they offer several key advantages. They can be generated from multiple somatic cell sources (e.g., peripheral blood mononuclear cells, skin fibroblasts, etc.), retain the donor's genome, thus permitting functional assessment of individual genetic liability, and can be differentiated into diverse neuronal and glial phenotypes. These properties enabled the development of protocols to standardize in vitro modelling of human brain circuits and disease conditions, supporting targeted studies of risk gene variants and environmental exposures, as well as the development and testing of novel therapeutic pharmacological strategies. This is the case of mDA neurons of the human nigrostriatal and mesolimbic systems whose phenotype can be generated in vitro, at first starting from human ESCs, and more recently from human iPSCs, as detailed in this review. Over the past two decades numerous differentiation protocols have been reported, producing human mDA neurons that closely resemble caudal mDA neurons in vivo localized in substantia nigra and ventral tegmental area. In a previous study from the Meta-Research Innovation Center at Stanford (METRICS), the articles published in the period 2004-2017 were systematically evaluated (Marton and Ioannidis, 2019). The authors identified 75 publications with protocols, but only 35% of them (n = 26) were replicated and used again in other articles. The inclusion criteria for defining protocols reporting human iPSC/ESC-differentiated DA neurons were: (a) expression of neural lineage markers, (b) exit the cell cycle, (c) expression of Tyrosine Hydroxylase (TH) or other DA neuron markers, and (d) evidence of proper neuronal morphology in culture. The protocols were also classified in Novelty Category A articles, involving protocols with innovative content, and Novelty Category B articles, describing modifications from the original protocols (Marton and Ioannidis, 2019). In their analysis, these two categories were mixed, since the main goal of the study was to assess the impact of innovations into the Stem Cell research community. Based on the 15-year experience of our laboratory in iPSCs differentiation in mDA neurons, here we propose a pragmatic review that highlights protocols that introduced innovative technical steps in the differentiation process from pluripotency to caudal mDA neuron phenotype leading to an impact on either percentage of DA neurons, or authenticity, or procedural optimization, or replicability, therefore partially resembling the Novelty Category A of Marton and Ioannidis (2019). Notably, a pragmatic review (Pragmatic Review - York Health Economics Consortium, 2025) adapts the conventional systematic review process due to limited time, resources, and, as in this case, the availability of specific knowledge and expertise. Therefore, some steps of the operational checklist from the PRISMA-P extension were omitted (Moher et al., 2015).

2. Methodology for articles selection and evaluation

The articles were searched from the PubMed database in June 2025 and revised in December 2025 using keywords such as: 'Human Pluripotent Stem Cells', 'Differentiation into Midbrain Dopaminergic Neurons' in the period 2004-2025, resulting in 332 articles. By filtering using the keyword 'Protocol', the articles were reduced to 108. These articles were collected, read, and analyzed by 2 members of the team with 5 and 15 years of experience in iPSCs differentiation into mDA neurons, respectively, implementing the same basic criteria of Marton and Ioannidis (2019). Regarding the innovative aspects, the selection criteria here applied were aimed to identify articles with differentiation protocols that introduced novel technical steps in the differentiation process to mDA neurons, resulting in improvement of at least one of the following outcome: (1) the yield as percentage of DA neurons, (2) the authenticity, i.e., the similarity vs. mDA neurons described in vivo, (3) the cost/benefit efficiency of the laboratory procedures, (4) the method replicability, as expressed by the presence quotations in the NCBI database that were not from the same laboratory or authors. Articles reporting protocols with minor modifications vs. the original differentiation protocols, seen as obvious or marginal, were excluded. In fact, the focus was on the presence of technical improvements in the differentiation procedures of neurodevelopmental relevance, at variance with articles focused on improving the phenotypic descriptors of mDA neurons in various differentiation stages (e.g., patch-clamp electrophysiology, single-cell genomic profiling, etc.). Moreover, in this review we included protocols that implemented both 2-dimensional (2D) and 3-dimensional (3D)/organoid cultures for differentiation. We excluded protocols aimed to obtain human DA neurons using viral vector-mediated forced expression of ventral midbrain determinants by random integration of constructs in the genome (Chung et al., 2009; Sánchez-Danés et al., 2012). We also excluded the direct conversion of human fibroblasts in DA neurons, also defined as Induced Dopaminergic (iDA) neurons (Caiazzo et al., 2011). These technologies, predating the CRISPR/Cas9 more recent approaches (Carter et al., 2020), resulted in iDA neurons with important transcriptional differences vs. in vivo mesencephalic DA neurons (Xia et al., 2016), or carrying some disruption of their typical neurodevelopment patterning process (Rifes et al., 2024). Additional selection criteria for optimal protocols were related to the level of characterization of mature mDA neurons, including: (a) the presence of TH-immunoreactivity neuronal profiles assessed as percentage counts vs. total cells, (b) the co-expression of maturity and midbrain caudal markers. e.g., either Dopamine Transporter (DAT), or G-Protein–Regulated Inward-Rectifier Potassium Channel 2 (GIRK), or Nuclear Receptor-Related 1 Protein (NURR1), (c) the evidence of functional dopamine uptake/release, (d) the presence of electrophysiological spontaneous firing <10 Hz, and (e) the evidence of survival and synaptic interconnectivity after in vivo transplantation. The selection produced 12 articles with protocols for 2D culture and 11 articles with protocols for 3D/organoid cultures. These protocols are summarized in Tables 1 and 2 that included details on the innovative technological step, the characterization of the maturity stages of mDA neurons with caudal midbrain phenotype based on biomarkers, on uptake/release of dopamine, on the electrophysiology profile and on the percentage yield vs. total neurons. Improvements in simplicity and efficiency of the procedure, if present, were described in the text. Replicability and impact were indirectly provided by the number of citations (Table 1).

3. In vitro mimicking the developmental processes of midbrain DA neurons

Midbrain DA neuron differentiation protocols for ESCs and iPSCs were originally designed to recapitulate the developmental mechanisms initially explored and described in the embryonic mouse ventral midbrain, where morphogens such as Sonic Hedgehog Protein (SHH), WNT/β-catenin and Fibroblast Growth Factor 8 (FGF8), together with

Table 1A
Innovative aspects of 2D protocols for mDA neuron differentiation.

Authors	Cell sources	Critical contributions	[1]Citations
Perrier et al. (2004)	Human ESCs	Differentiation of ESCs into mDA neurons via neural rosettes on stromal feeders, followed by sequential patterning with SHH/FGF8.	894
Sonntag et al. (2007)	Human ESCs	Application of Noggin (a bone morphogenetic protein antagonist) to induce neuroectodermal specification and enhance mDA neuron yield from ESCs via neural rosette formation.	225
Cooper et al. (2010)	Human ESCs Human iPSCs	Optimization of mDA neurons differentiation via neural rosette formation in feeder-free condition by: (1) early exposure to low-dose retinoic acid to enhance regional identity of NPs; (2) administration of SHH to increase FOXA2-positive midbrain FP progenitors; (3) early treatment with FGF8α plus WNT1 to promote differentiation into FOXA2-positive mDA neurons.	195
Swistowski et al. (2010)	iPSCs	Generation of mDA neurons from iPSCs via EBs formation and neural rosettes differentiation in xeno-free conditions.	283
Kriks et al. (2011)	Human ESCs iPSCs	Differentiation of mDA neuron from iPSCs via FP induction using CHIR99021 (GSK3β inhibitor) to activate WNT signaling and purmorphamine to enhance SHH pathway activity alongside recombinant SHH.	1591
Xi et al. (2012)	Human ESCs Human iPSCs Rhesus monkey iPSCs	Optimization of CHIR99021 concentration and timing for mDA neuron generation via FP induction to achieve midbrain regional specification.	186
Kirkeby et al. (2012)	Human ESCs	Introduction of a feeder-free EB-based differentiation protocol consisting of FP induction employing CT99021 (an alternative GSK3β inhibitor to CHIR99021) for WNT signaling activation.	546
Sundberg et al. (2013)	Human ESCs Human iPSCs Non-human primate iPSCs	$NCAM^{+}/CD29^{low}$ cell sorting approach for enriching mDA neurons derived from iPSCs via FP induction. Transplantation into 6-OHDA-lesioned rat and non-human primate striatum showed graft survival at one-year post-transplantation in one primate without immunosuppressive therapy.	206
Doi et al. (2014)	Human iPSCs	CORIN-based cell sorting for efficient isolation of iPSC-derived mDA progenitors expressing FOXA2/LMX1A floor plate markers. Differentiation via FP induction on recombinant laminin-511 (instead of Matrigel) enhanced cell survival and mDA neuron differentiation under xeno-free, scalable conditions.	368
Fedele et al. (2017)	Human iPSCs	FP induction protocol for generating and expanding homogeneous midbrain FP progenitor that retains efficient DA neurogenic potential over multiple passages (>6) and can be cryobanked for future use.	41
Nolbrant et al. (2017)	Human iPSCs	Optimized 16-day protocol adapted from the Kirkeby et al. (2012) ventral midbrain method. It standardizes CHIR, SHH and FGF8β timing and dosing across multiple iPSC lines to obtain 80–95% FOXA2/LMX1A/OTX2 caudal ventral midbrain progenitors. The protocol is GMP-compatible, xeno-free, and includes a defined QC marker panel.	190
Kim et al. (2021)	Human iPSCs	Optimization of Kriks protocol employing a two-step WNT signaling activation strategy with a boost phase of CHIR99021 (7.5 μM) from day 4 to day 10 to enhance midbrain marker expression and mDA neuron yield.	144

2D: 2-Dimensional; **3D**: 3-Dimensional; **6-OHDA**: 6-Hydroxydopamine; **CD29**:: integrin b-1; **DA**: Dopaminergic; **EBs**: Embryoid Bodies; **ESCs**: Embryonic Stem Cells; **FACS**: Fluorescence-Activeted Cell Sorting; **FGF8**: Fibroblast Growth Factor 8; **FOXA2**: Forkhead Box A2; **FP**: Floor Plate; **GMP**: Good Manufacturing Practice; **GSK3β**: Glycogen Synthase Kinase 3 Beta; **iPSCs**: Induced Pluripotent Stem Cells; **LMX1A**: LIM Homeobox Transcription Factor 1-Alpha; **LRRK2**: Leucine-Rich Repeat Kinase 2; **mDA**: Midbrain Dopaminergic; **NCAM**: Neural Cell Adhesion Molecule; **NPs**: Neural precursors; **OTX2**: Orthodenticle Homeobox 2; **PDMS**: Polydimethylsiloxane; **QC**: Quality Control; **scRNA-seq**: Single-Cell RNA Sequencing; **SHH**: Sonic Hedgehog Protein; **TH**: Tyrosine Hydroxylase.
[1] Citations assessed in Scopus and update to October 2025.

transcription factors including LIM Homeobox Transcription Factor 1-alpha/beta (LMX1A/B), Forkhead Box A2 (FOXA2), Msh Homeobox 1 (MSX1), Neurogenin (NGN2), NURR1 and Pituitary Homeobox 3 (PITX3), act sequentially to specify progenitors, immature neurons and, later, the mature mDA ventro-caudal midbrain subtypes (Arenas, 2014; Arenas et al., 2015; Hegarty et al., 2013; Volpicelli et al., 2020). More recently, single cell studies of human fetal ventral midbrain and organoid-like cultures, as well as human pluripotent stem cell–based models, have mapped the corresponding human pathways and uncovered both conserved patterning cues (i.e., SHH, WNT, FGF8 and the FOXA2–LMX1A–NURR1 axis), including some human-specific markers and trajectories that were not predicted from mouse studies. La Manno et al. (2016) provided the first comprehensive study of human and mouse ventral midbrain development, defining progenitor and neuronal subtypes and highlighting species differences in timing, proliferation and mDA lineage progression (La Manno et al., 2016), while Birtele et al. (2022) extended this work by profiling human fetal ventral midbrain tissue together with 3D/organoid-like cultures, demonstrating that these cultures can generate and maintain mature human DA neurons and revealing human-enriched DA subclusters and genes, including primate-specific markers (Birtele et al., 2022). Together, these studies show that additional human-enriched genes and cell states are emerging, creating an opportunity to refine growth-factor and small-molecule signaling regimens to optimize mDA differentiation protocols. In the coming years, these human data sets are expected to be increasingly used to guide adjustments in signal timing, dose, and combinations in existing protocols to better reproduce human midbrain development in vitro. Over time, a variety of mDA differentiation protocols have been developed that mainly differ in which of the described 'signals' are used, in what order they are applied, and for how long they are maintained in culture. From the mid-2000s until the advent of midbrain organoid protocols in the mid-2010s, these strategies were implemented almost exclusively in 2D cultures, in which ESCs or iPSCs are grown as adherent monolayers on coated plastic or glass, in some cases on top of stromal feeder cells, and exposed to patterning factors in a relatively homogeneous environment. These cultures allow the differentiation up to mature mDA phenotypes with functional synaptic connectivity organized in random networks, as shown by calcium imaging and electrophysiology (Comella-Bolla et al., 2020; Hartfield et al.,

Table 1B
Innovative aspects of 3D protocols for mDA neuron differentiation.

Authors	Cell sources	Critical contributions	[1]Citations
Tieng et al. (2014)	Human ESCs and human iPSCs	Generation of 3D midbrain-like organoids yielding >60% TH + mDA neurons within 3 weeks. Enhanced neuronal maturation by modulation of Notch signaling with γ-secretase inhibitors. The protocol utilizes FP induction followed by engendered neural tissue formation on hydrophilic substrates.	104
Jo et al. (2016)	Human ESCs and human iPSCs	Generation of 3D midbrain-like organoids from ESCs and human iPSCs via EBs formation and FP induction to obtain functional mDA neurons releasing dopamine and containing neuromelanin-like granules.	665
Qian et al. (2016)	Human iPSCs	Application of mini-bioreactors and regional patterning factors (including FP induction for midbrain) to generate region-specific 3D brain organoids (forebrain, midbrain, hypothalamus) that recapitulate human-specific outer radial glia layers and progenitor zone architecture.	1731
Monzel et al. (2017)	Human iPSCs	Derivation of 3D midbrain-like organoids from neuroepithelial stem cells containing spatially organized dopaminergic neurons with functional synaptic connections and electrophysiological activity, along with glia (astrocytes, oligodendrocytes) and myelinated neurites.	338
Smits et al. (2019)	Human iPSCs	Differentiation of 3D midbrain-like organoids from expandable midbrain FP progenitors in ultra-low attachment round bottom plates that recapitulate dopamine development and dopamine secretion This approach was utilized to generate 3D midbrain-like organoids from Parkinson's disease patients carrying the LRRK2-G2019S mutation, which faithfully recapitulate key disease-relevant phenotypes.	255
Nickels et al. (2020)	Human ESCs and human iPSCs	Development of a standardized 3D midbrain-like organoid protocol from human iPSCs derived midbrain NPs in ultra-low adhesion plates under shaking conditions to minimize necrotic core formation batch variability while preserving dopaminergic neuron and astrocyte differentiation subsequently applied to establish a 6-OHDA neurotoxin-based Parkinson's disease model.	88
Kim et al. (2021)	Human ESCs and human iPSCs	Enrichment of neural stem cells from human midbrain-like organoids that can be engrafted in a rodent Parkinson's disease model.	43
Sarrafha et al. (2021)	Human iPSCs	Establishment of a high-throughput 3D organoid differentiation protocol from human iPSCs that yields uniform mDA neuron organoids and includes reporter lines to enable FACS-based enrichment of TH + cells.	13
Fiorenzano et al. (2021)	Human iPSCs	Derivation of 3D ventral midbrain organoids from EBs using spider-silk/laminin-511 scaffolding in Matrigel-embedded U-bottom plates to achieve uniform mDA neuron differentiation. scRNA-seq identified three mDA neuron subtypes.	94
Sozzi et al. (2022)	Human iPSCs	Generation of 3D midbrain-like organoids from iPSCs through EBs formation, Matrigel embedding, and patterned differentiation (dual SMAD inhibition/SHH/CHIR99021) yielding functionally mature dopaminergic neurons with neuromelanin.	19
Reumann et al. (2023)	Human ESCs and human iPSCs	Generation of midbrain-striatum-cortical assembloids from EBs in PDMS molds under shaking culture that develop functional long-range dopaminergic projections, model circuit formation, dopamine release, progenitor engraftment, and drug perturbations with cocaine, enabling human disease modeling, pharmacological studies.	53

2D: 2-Dimensional; **3D**: 3-Dimensional; **6-OHDA**: 6-Hydroxydopamine; **CD29**:: integrin b-1; **DA**: Dopaminergic; **EBs**: Embryoid Bodies; **ESCs**: Embryonic Stem Cells; **FACS**: Fluorescence-Activeted Cell Sorting; **FGF8**: Fibroblast Growth Factor 8; **FOXA2**: Forkhead Box A2; **FP**: Floor Plate; **GMP**: Good Manufacturing Practice; **GSK3β**: Glycogen Synthase Kinase 3 Beta; **iPSCs**: Induced Pluripotent Stem Cells; **LMX1A**: LIM Homeobox Transcription Factor 1-Alpha; **LRRK2**: Leucine-Rich Repeat Kinase 2; **mDA**: Midbrain Dopaminergic; **NCAM**: Neural Cell Adhesion Molecule; **NPs**: Neural precursors; **OTX2**: Orthodenticle Homeobox 2; **PDMS**: Polydimethylsiloxane; **QC**: Quality Control; **scRNA-seq**: Single-Cell RNA Sequencing; **SHH**: Sonic Hedgehog Protein; **TH**: Tyrosine Hydroxylase.
[1] Citations assessed in Scopus and update to October 2025.

2014). The 2D culture models of this type are still widely used to investigate molecular and cellular mechanisms, as well as for medium-throughput drug screening. More recently, 3D culture models have been developed to better approximate the architecture of tissues and organs. In these systems, cells self-organize into brain region-specific organoid-like structures, allowing growth and interaction in an anatomically plausible and physiologically relevant environment, differentiating into more in vivo-like neuronal diversity, more realistic cell–cell synaptic interactions and extracellular gradients, and the possibility to incorporate organoid from other brain regions, or additional cell types, such as microglia (Fig. 1) (Kim et al., 2020; Sabate-Soler et al., 2022). These conceptual differences between 2D and 3D systems underline the protocol variations discussed in the following sections.

3.1. Protocols for midbrain DA neurons differentiation in 2D cultures

Building on the foundational work described in the preceding section, early efforts to generate mDA neurons from pluripotent stem cells primarily relied on 2D culture systems. We identified and systematically analyzed twelve protocols, and their main features are summarized in Tables 1A and 2A. Protocols for the differentiation of human iPSCs into mDA neurons were initially adapted from methods previously optimized for human ESCs. Perrier et al. (2004) first described the generation of mDA neurons from human ESCs through the formation of neural rosettes. In this system, neuroectodermal differentiation was induced by co-culture with stromal feeder cells, followed by the sequential application of defined patterning factors (Fig. 2A) (Perrier et al., 2004). Sonntag et al. (2007) maintained stromal co-culture to promote neuroectodermal differentiation and introduced Noggin to enhance the

Table 2A
DA neuron marker profiles across 2D differentiation protocols.

	Neural induction markers		Neural differentiation markers				Functional phenotype		Additional information		Maturation
Protocol	FOXA2	LMX1A	TH	DAT	NURR1	GIRK2	Electrophysiology	Release/ Uptake of dopamine	Other neuronal/ glial population	In vivo studies	Stage of differentiation reached
Perrier et al. (2004)	n.a.	+ n.q. ICC (day 42)	64-79% /TUJ1$^+$ ICC (day 50) + RT-PCR (day 28, 35, 42, 50)	n.a.	+ RT-PCR (day 42, 50)	n.a.	Depolarization-induced action potentials detected in 65% of the neurons; blocked TTX. (day 60-70)	Basal and KCl induced release of dopamine. HPLC (Day 50)	~5% serotonin$^+$/ total cells. ICC (day 50) 1-2 % GABA$^+$/ total cells. ICC (day 50)	n.a.	Day 60-70
Sonntag et al. (2007)	n.a.	+ RT-PCR (day 21, 30, 37 and 42)	22,3%/total cells ICC (day 49) + RT-PCR (day 42) + qPCR (day 37 and 42)	n.a.	+ RT-PCR (day 30, and 42)	+ n.q. ICC	n.a.	n.a.	1,4% GFAP$^+$/total cells. ICC (day 49)	Day 42 neurons were transplanted into the striatum of 6-OHDA lesioned rat brain.	Day 49
Cooper et al. (2010)	~15%/total cells. ICC (day 19)	n.a.	~2% (co-exp. βTUB/ FOXA2)/ total cells. ICC (day 49)	n.a.	n.a.	+ n.q. ICC (day 49)	n.a.	n.a.	n.a.	n.a.	Day 49
Swistowski et al. (2010)	n.a.	n.a.	~30% ± 5%/total cells. ICC (day 35) + qPCR (day 35)	+ q-PCR (day 35)	+ q-PCR (day 35)	~100%/TH$^+$ ICC (day 35) + qPCR (day 35)	n.a.	n.a.	n.a.	Day 20 post NSCs stage DA neurons were transplanted into 6-OHDA lesioned rat brain.	Day 35
Kriks et al. (2011)	~80%/total cells. ICC (day 11) + qPCR (day 3, 5, 7, 11, 13, 25)	~60%/total cells. ICC (day 11) + qPCR (day 3, 5, 7, 11, 13, 25)	~75%/total cells. ICC (day 50)	+ n.q. ICC (day 80)	~50%/total cells ICC (day 50)	+ n.q. ICC (day 80)	Spontaneous spikes at slow rate (1–3 Hz) accompanied by slow membrane potential oscillation. (day 80)	Dopamine and its metabolites DOPAC and HVA release. HPLC (day 65)	Few GABA$^+$ and 5HT$^+$ neurons. ICC (day 50)	Day 25 DA neurons were transplanted into adult mice and 6-OHDA lesioned NOD-SCID IL2Rgc null mice. Pilot grafting in adult MPTP-lesioned rhesus monkeys.	Day 80
Xi et al. (2012)	92,6 ± 3,8%/total cells. ICC (day 18)	~95%/ FOXA2$^+$ ICC (day 18)	43,6% ± 6,2%/total cells. ICC (day 35)	n.a.	95,3 ± 2,4%/TH$^+$ ICC (day 35)	56,3 ± 6,7%/TH$^+$ ICC (day 35)	Spontaneous action potentials accompanied by slow membrane potential oscillations. Spontaneous postsynaptic currents partially blocked by CNQX and fully blocked by combination of CNQX and bicuculline. (day 70)	n.a.	2,4 ± 1,2% 5HT$^+$/ total cells. ICC (day 35) 5,3 ± 2,7% GABA$^+$/total cells. ICC (day 35)	n.a.	Day 70
Kirkeby et al. (2012)	+n.q. ICC (day 42) 81% (co-	81 % (co-exp. FOXA2)/	+n.q. ICC (day 42)	n.a.	+ n.q. ICC (6	+ n.q. ICC (18 weeks after grafting)	Spontaneous postsynaptic currents blocked by NBQX and D-	n.a.	n.a.	VM progenitors transplanted into 6-	Day 42

(*continued on next page*)

Table 2A (*continued*)

	Neural induction markers		Neural differentiation markers				Functional phenotype		Additional information		Maturation
Protocol	FOXA2	LMX1A	TH	DAT	NURR1	GIRK2	Electrophysiology	Release/ Uptake of dopamine	Other neuronal/ glial population	In vivo studies	Stage of differentiation reached
	exp. LMX1A)/ total cells. ICC (6 weeks after grafting) + qPCR	total cells. ICC (6 weeks after grafting) + qPCR	+ n.q. ICC (6 weeks after grafting)		weeks after grafting)		AP5, but not by picrotoxin. (day 35)			OHDA lesioned rat striatum.	
Sundberg et al. (2013)	>50-70%/ total cells. ICC (day 30 after $NCAM^+$/ $CD29^{low}$ sorting) + qPCR (day 25-30 after $NCAM^+$/ $CD29^{low}$ sorting)	+ qPCR (day 25-30 after $NCAM^+$/ $CD29^{low}$ sorting)	40/50%/ total cells. ICC (day 30 after $NCAM^+$/ $CD29^{low}$ sorting) + qPCR (day 25-30 after $NCAM^+$/ $CD29^{low}$ sorting)	n.a.	+ qPCR (day 25-30 after $NCAM^+$/ $CD29^{low}$ sorting)	+ qPCR (day 25-30 after $NCAM^+$/ $CD29^{low}$ sorting)	n.a.	n.a.	<5% $serotonin^+$/ TH^-/total cells. ICC (day 30)	Unsorted and $NCAM^+$/ $CD29^{low}$ sorted DA neurons transplanted into striatum of 6OHDA lesioned rats and into the putamen of MPTP-lesioned cynomolgus Macaque.	Day 30
Doi et al. (2014)	75,5 % ± 8,2% (co-exp. LMX1A)/ total cells. ICC (day 12 after $CORIN^+$ sorting) ~80%/total cells ICC (day 28 after $CORIN^+$ sorting) + qPCR (day 12, 21, 28 and 42)	75,5 % ± 8,2% (co-exp. FOXA2)/ total cells. ICC (day 12 after $CORIN^+$ sorting) + qPCR (day 12, 21, 28 and 42)	42% ± 4,4%/total cells. ICC (day 42 after $CORIN^+$ sorting) + qPCR (day 12, 21, 28 and 42)	n.a.	19,9 ± 6.9%/total cells. ICC (day 42 after $CORIN^+$ sorting) + qPCR (day 12, 21, 28 and 42)	+ n.q. ICC (day 42)	Presence of action potential. (day 42)	Dopamine and DOPAC, release. HPLC (day 56)	1,2 ± 0,8% $serotonin^+$/total cells. ICC (16 weeks after vivo transplantation)	Unsorted and $CORIN^+$ cells at day 28 were injected into putamen of 6-OHDA-lesioned rats.	Day 56
Fedele et al. (2017)	90-95% (co-exp. LMX1A)/ total cells. ICC (day 11)	90-95% (co-exp. FOXA2)/ total cells. ICC (day 11)	8,6% ± 2,45% FACS (day 20) + RT-PCR and qPCR	+ RT-PCR and qPCR	+ n.q. ICC (day 30)	+ RT-PCR and qPCR + n.q ICC (day 80)	31.3% of neurons with HCN-mediated currents. All neurons with HCN currents had sag response. (day 50)	Dopamine release. LC-MS (day 40, peaking at day 60)	n.a.	FP progenitors were transplanted into VM of mouse embryos *in utero*.	Day 80
Nolbrant et al. (2017)	+ n.q. ICC (day 14-16) + qPCR (day 16)	+ n.q. ICC (day 14 -16) + qPCR (day 16)	+ n.q. ICC (day 44-50)	n.a.	n.a.	n.a.	n.a.	n.a.	Absence of glial differentiation (GFAP).	Day 16 DA progenitors were transplanted into rat striatum.	Day 42-50

(*continued on next page*)

Table 2A (*continued*)

Protocol	Neural induction markers		Neural differentiation markers				Functional phenotype		Additional information		Maturation
	FOXA2	LMX1A	TH	DAT	NURR1	GIRK2	Electrophysiology	Release/ Uptake of dopamine	Other neuronal/ glial population	In vivo studies	Stage of differentiation reached
Kim et al. (2021)	90-95%/ total cells. ICC (day 11) + n.q. ICC (day 60 and 75) + qPCR (day 11, 15, 20, and 60)	+ n.q. ICC (day 11, 60 and 75) + qPCR (day 11, 15, 20, 30 and 60)	+ n.q. ICC (day 60 and day 75)	n.a.	+ qPCR (day 20, 30 and 60) + ICC (day 75)	+ qPCR (day 30 and 60) 65%/TH$^+$ ICC (6 months after in vivo transplantation)	58% of DA neurons showed moderate spiking and 21% burst spiking, with multiple action potentials, spike-frequency adaptation, and membrane currents typical of mature neurons. (day 75)	Dopamine release. HPLC (day 60)	<1% 5HT$^+$/total cells. ICC (5.5 months after in vivo transplantation). Few GFAP$^+$ cells. ICC (5.5 months after in vivo transplantation)	DA neuron precursors at day 16 were transplanted into striatum of 6-OHDA-lesioned rat.	Day 75

2D: 2-dimensional; **3D**: 3-dimensional; **5HT**: 5-hydroxytryptamine; **6-OHDA**: 6-Hydroxydopamine; **βTUB**: βIII-Tubulin; **CD29**: integrin b-1; **ChAT**: Choline Acetyltransferase; **CNQX**: 6-cyano-7-nitroquinoxaline-2,3-dione; **co-exp.** co-expression; **COL1A**:1 Collagen Type I Alpha 1 Chain; **DA**: Dopaminergic; **D-AP5**: D(−)-2-Amino-5-phosphonovaleric acid; **DAT**: Dopamine Transporter; **DOPAC**: 3,4-dihydroxy-phenylacetic acid; **ELISA**: Enzyme-Linked Immunosorbent Assay; **FACS**: Fluorescence-Activated Cell Sorting **FOXA2**: Forkhead Box A2; **FP**: Floor Plate; **GABA**: Gamma-Aminobutyric Acid; **GFAP**: Glial Fibrillary Acidic Protein; **GIRK2**: G-protein-regulated inward-rectifier potassium channel 2; **HCN**: Hydrogen Cyanide; **HPLC**: High-Pressure Liquid Chromatography; **HVA**: Homovanillic Acid; **ICC**: Immunocytochemistry; **KCL**: Potassium Chloride **LC-MS**: Liquid Chromatography-Mass Spectrometric; **LMX1A**: LIM Homeobox Transcription Factor 1-alpha; **MAP2**: Microtubule-Associated Protein 2; **MPTP**: 1-methyl-4-phenyl-1,2,3,6-tetrahydropyridine; **n.a.** not assessed; **n.q.** not quantified; **NBQX**: 2,3-Dihydroxy-6-nitro-7-sulfamoyl-benzo(F)quinoxaline; **NCAM**: Neural Cell Adhesion Molecule; **NSC**: Neural Stem Cells; **NURR1**: Nuclear Receptor-Related 1 Protein; **O4**: Oligodendrocyte Marker 4; **OLIG1**: Oligodendrocyte Transcription Factor 1; **OLIG2**: Oligodendrocyte Transcription Factor 2; **PDGFRα**: Platelet Derived Growth Factor Receptor alpha; **qPCR**: quantitative PCR; **RT-PCR**: Reverse Transcription-Polymerase Chain Reaction; **S100B**: S100 calcium binding protein B; **scRNA-seq**: single-cell RNA sequencing **TH**: Tyrosine Hydroxylase; **TTX**: Tetrodotoxin; **VGLUT1**: Vesicular Glutamate Transporter 1; **VGLUT2**: Vesicular Glutamate Transporter 2; **VM**: Ventral Midbrain.

homogeneity of rosette-like structures and improve the efficiency of differentiation into TH-positive neurons. Despite these advances, the resulting neurons lacked a stable ventral midbrain identity (Sonntag et al., 2007). Cooper et al. (2010) overcame this limitation by introducing three key modifications: (i) early exposure to retinoic acid to enhance regional patterning of progenitors, (ii) use of the recombinant SHH variant SHH-C24II to increase the generation of FOXA2-positive neural progenitors, and (iii) replacement of FGF8β with FGF8α, which promoted efficient differentiation of FOXA2-positive Floor Plate (FP) progenitors into mature FOXA2-positive mDA neurons (Cooper et al., 2010). In parallel, Swistowski et al. (2010) established a fully xeno-free differentiation system that generated A9-type caudal midbrain DA neurons through embryoid bodies (EBs) and rosette formation (Swistowski et al., 2010). Across 2D paradigms using neural rosette intermediates, maximal differentiation efficiency reached approximately 30% TH-positive neurons, as quantified by immunocytochemistry. In parallel with these developments, a major conceptual shift came with the introduction of the dual-SMAD inhibition approach by Chambers et al. (2009), who demonstrated that simultaneous blockade of Bone Morphogenetic Protein (BMP) and Transforming Growth Factor-beta (TGF-β) signalling via Noggin and SB431542 was sufficient to induce neural conversion, eliminating the need for stromal cells or EBs formation (Chambers et al., 2009). Subsequently, Kriks et al. (2011) improved this method by incorporating CHIR99021, a potent Glycogen Synthase Kinase 3 beta (GSK3β) inhibitor that activates canonical WNT signalling. Exposure to CHIR99021 between days 3 and 11 of differentiation markedly increased the proportion of LMX1A/FOXA2 double-positive progenitors, yielding up to a maximum of 75% TH-positive neurons (Fig. 2B) (Kriks et al., 2011). The co-expression of FOXA2 and LMX1A represented a significant step toward generating authentic mDA neurons with ventral midbrain identity, as assessed using specific markers and electrophysiologic profile. This finding was supported by Xi et al. (2012), who demonstrated that early exposure to narrowly titrated CHIR concentrations (0.2–0.6 μM) was critical for efficient midbrain specification of both ESCs and iPSCs (Xi et al., 2012). Kirkeby et al. (2012) integrated dual-SMAD inhibition with EB-based differentiation and showed that combining potent GSK3β inhibition with SHH-C24II efficiently directed cultures toward the ventral midbrain fate. Importantly, the authors implemented a chemically defined, xeno-free culture environment devoid of serum, serum replacements, and Matrigel, enhancing reproducibility and translational potential (Kirkeby et al., 2012). Nolbrant et al. (2017) from the same group further refined this system by standardizing progenitor differentiation to a 16-day schedule, thereby reducing phenotypic heterogeneity and enabling quality control compatible with clinical-grade manufacturing (Nolbrant et al., 2017). The subsequent improvements were mainly aimed to enhance matrix substrate definitions and progenitor enrichments. Doi et al. (2014) developed a xeno-free substrate using recombinant E8 fragments of laminin-511, which supported mDA neuron differentiation more effectively than Matrigel. They also introduced CORIN as a FP marker to isolate FOXA2/LMX1A-positive progenitors (Doi et al., 2014). Fedele et al. (2017), building on the work of Kriks et al. (2011), produced a protocol to enable the generation and expansion of homogeneous midbrain FP progenitors that retained robust mDA neurogenic potential over multiple passages. These progenitors could be cryopreserved without loss of functionality and subsequently differentiated into mature mDA neurons that display the expected morphologic, biomarker expression, and electrophysiological properties (Fedele et al., 2017). Cell purification strategies were applied to increase the yield of mDA neurons. Sundberg et al. (2013) employed Fluorescence-Activated Cell Sorting (FACS) using NCAM$^+$/CD29^{low} gating to isolate neuron-enriched populations, increasing TH-positive cells from approximately 20% in unsorted cultures to 40–50% post-sorting (Sundberg et al., 2013). Throughout all these 2D differentiation paradigms, modulation of the WNT signalling pathway with CHIR99021 remained central in specifying midbrain identity. However, Kirkeby

Table 2B
DA neuron marker profiles across 3D differentiation protocols.

	Neural induction markers		Neural differentiation markers				Functional phenotype		Additional information		Maturation
Protocol	FOXA2	LMX1a	TH	DAT	NURR1	GIRK2	Electrophysiology	Release/Uptake of dopamine	Other neuronal population	Neuromelanin	Stage of differentiation reached
Tieng et al. (2014)	~ 80%/total cells. ICC (day 21, after dissociation and plating onto 2D for one week) + RT-PCR (day 30)	~ 80%/total cells. ICC (day 21 after dissociation and plating onto 2D for one week) + RT-PCR (day 30)	~ 60%/total cells. ICC (day 21, after dissociation and plating onto 2D for one week) + qPCR (day 30)	n.a.	~ 60%/total cells. ICC (day 21, after dissociation and plating onto 2D for one week) + RT-PCR (day 30)	n.a.	Individual or bursting extracellular action potentials.	Dopamine release. HPLC	GFAP$^+$ and VGLUT1$^+$ cells. ICC (day 51)	n.a.	Day 50
Jo et al. (2016)	~ 35%/total cells. ICC (day 45) 81%/LMX1A$^+$ ICC (day 45)	38%/total cells. ICC (day 45) + qPCR (day 30 and 60)	54%/FOXA2$^+$ ICC (day 45) 58%/LMX1A$^+$ ICC (day 45) 22%/MAP2$^+$ FACS (day 60) + qPCR (day 30 and 60)	29%/TH$^+$ ICC (day 60)	+ n.q. ICC (day 35) + qPCR (day 30 and 60)	+ n.q. ICC (day 60)	Spontaneous firing at slow rate (avg. 2.78 Hz). (day 65)	Dopamine release. HPLC (day 28, 35, 49, 63 and 91)	GABA$^+$ ChAT$^+$ and 5HT$^+$ cells. ICC (day 35)	Neuromelanin inclusions. (day 60-146)	Day 146
Qian et al. (2016)	+ n.q. ICC (day 18 in 3D structure) 95 ± 1%/total cells. ICC (day 65 after organoid dissociation and plating onto 2D for 5 days)	n.a.	+ n.q. ICC (day 38 in 3D structure) 55 ± 4%/total cells. ICC (day 65 after organoid dissociation and plating onto 2D for 5 days)	+ n.q. ICC (day 56 in 3D structure)	+ n.q. ICC (day 56 in 3D structure)	n.a.	n.a.	n.a.	n.a.	n.a.	Day 65
Monzel et al. (2017)	64% ± 2,4% (co-exp. LMX1A/TH) Flow-cytometry (day 61) + ICC (day 61)	64% ± 2,4% (co-exp. FOXA2/TH) Flow-cytometry (day 61) + ICC (day 61)	64% ± 2,4% (co-exp. FOXA2/ LMX1A) Flow-cytometry (day 61) + ICC (day 27 and 61) + qPCR	+ n.q. ICC (day 61) + qPCR	+ n.q. ICC (day 30 and 61)	+ n.q. ICC (day 61)	Spontaneous mono-/ biphasic spikes and network synchronicity reduced by quinpirole. (day 82-84)	Dopamine expression. ICC (day 50)	4% S100B$^+$ astrocytes. ICC (day 61) O4$^+$ oligodendrocytes. ICC (day 61)	Neuromelanin inclusions. (day 149)	Day 149
Smits et al. (2019)	+ n.q. ICC (day 35 and 70) + qPCR (35 and 70)	+ n.q. ICC (day 70) + qPCR (35 and 70)	54,12 ± 3,5%/total cells. ICC (day 70) + qPCR (35 and 70)	+ n.q. ICC (day 70)	n.a.	+ ICC (day 35)	Slow spontaneous firing (9 ± 2 Hz). 81% of the cells displayed sodium currents and 100% potassium currents. (organoids dissociated at day 60-65 and patch clamp recording carried	Quantification of dopamine. ELISA (day 35 and 70)	n.a.	Neuromelanin inclusion. (day 255)	Day 255

(*continued on next page*)

Table 2B (*continued*)

	Neural induction markers		Neural differentiation markers				Functional phenotype		Additional information		Maturation
Protocol	FOXA2	LMX1a	TH	DAT	NURR1	GIRK2	Electrophysiology	Release/Uptake of dopamine	Other neuronal population	Neuromelanin	Stage of differentiation reached
							out 5-15 days after dissociation)				
Nickels et al. (2020)	~ 54,01 ± 13,4 %/total cells. ICC (day 30)	n.a.	~ 80%/TUJ1^{+} ICC (day 30)	+ n.q. ICC (day 30)	n.a.	+ n.q. ICC (day 30)	n.a.	Dopamine expression. ICC (day 30)	10,51% S100B^{+}/ total cells. ICC (day 30) 7,13% GFAP^{+}/ total cells. ICC (day 30) VGLUT2^{+} and Serotonin^{+} cells. ICC (day 30)	n.a.	Day 30
Kim et al. (2021) [1]	+ n.q. ICC (day 25 and 40)	+ n.q. ICC (day 25 and 40)	+ n.q. ICC (day 40)	n.a.	+ n.q. ICC (day 40)	n.a.	n.a.	n.a.	n.a.	n.a.	Day 55
Sarrafha et al. (2021)	+ qPCR (day 15)	+ qPCR (day 15)	~ 12 %/total cells. ICC (day 21) 31,56% FACS (day30)	n.a.	+ qPCR (day 30)	+ qPCR (day 30)	n.a.	n.a.	GFAP^{+} cells. ICC (day 80)	Melanin inclusions. (day 200)	Day 200
Fiorenzano et al. (2021) [2]	+ n.q. ICC (day 21, 30 and 40) ~ 40 %/total cells. ICC (day 30) + qPCR (day 60)	+ n.q. ICC (day 30 in silk organoid)	+ n.q. ICC (day 50, 60 and 90) ~ 75 %/MAP2^{+} ICC (day 50) + qPCR (day 60)	+ n.q. ICC (day 90)	+ qPCR (day 60)	+ n.q. ICC (day 60)	Hyperpolarized resting potentials, mature Na+ and delayed-rectifier K+ currents, induced/ spontaneous action potentials, and DA-typical rebound depolarizations. (Day 90)	Real-time chronoamperometric measurements of dopamine exocytosis using a carbon-coated fiber.	GFAP^{+}, OLIG2^{+} and COL1A1^{+}/ PDGFRα^{+} cells. ICC (day 120)	Intracellular and extracellular neuromelanin. (day 120)	Day 120
Sozzi et al. (2022)	+ n.q. ICC (day 30) + qPCR (day 15, 30 and 60)	n.a.	+ n.q. ICC (day 60) + qPCR (day 30 and 60)	n.a.	+ qPCR (day 30 and 60)	n.a.	n.a.	n.a.	n.a.	Neuromelanin inclusions. (day 120 and 240)	Day 240
Reumann et al. (2023)	+ n.q. ICC (day 44) ~ 40 %/TH^{+} ICC (day 80) + qPCR (day 11, 16 and 30)	~ 30 %/TH^{+} ICC (day 80) + qPCR (day 11, 16 and 30)	+ n.q. ICC (day 44) ~ 40 -90 %/total cells ICC (day 80 in six lines) + scRNA-seq (day 60 in assembloids) + qPCR (day 16 and 30)	+ n.q. ICC (day 90 in assembloids)	+ qPCR (day 30)	~ 80 %/TH^{+} ICC (in assembloids)	Optogenetic stimulation of VM organoids elicited functional activity in the cortical and striatal projections of assembloids. (Day 140-170)	n.a.	Glutamatergic and GABAergic neurons scRNA-seq (day 60 in assembloids) OLIG1^{+} and S100B^{+} cells. scRNA-seq (day 60 in assembloids)	n.a.	Day 150

2D: 2-dimensional; **3D**: 3-dimensional: **5HT**: 5-hydroxytryptamine; **6-OHDA**: 6-Hydroxydopamine; **βTUB**: βIII-Tubulin; **CD29**: integrin b-1; **ChAT**: Choline Acetyltransferase; **CNQX**: 6-cyano-7-nitroquinoxaline-2,3-dione; **co-exp**. co-expression; **COL1A**:1 Collagen Type I Alpha 1 Chain; **DA**: Dopaminergic; **D-AP5**: D(−)-2-Amino-5-phosphonovaleric acid; **DAT**: Dopamine Transporter; **DOPAC**: 3,4-dihydroxy-phenylacetic acid; **ELISA**: Enzyme-Linked Immunosorbent Assay; **FACS**: Fluorescence-Activated Cell Sorting **FOXA2**: Forkhead Box A2; **FP**: Floor Plate; **GABA**: Gamma-Aminobutyric Acid; **GFAP**: Glial Fibrillary Acidic Protein; **GIRK2**: G-protein-regulated inward-rectifier potassium channel 2; **HCN**: Hydrogen Cyanide; **HPLC**: High-Pressure Liquid Chromatography; **HVA**: Homovanillic Acid; **ICC**: Immunocytochemistry; **KCL**: Potassium Chloride **LC-MS**: Liquid Chromatography-Mass Spectrometric; **LMX1A**: LIM Homeobox Transcription Factor 1-alpha; **MAP2**: Microtubule-Associated Protein 2; **MPTP**: 1-methyl-4-phenyl-1,2,3,6-tetrahydropyridine; **n.a.** not assessed; **n.q.** not quantified; **NBQX**: 2,3-Dihydroxy-6-nitro-7-sulfamoyl-benzo(F)quinoxaline; **NCAM**: Neural Cell Adhesion Molecule; **NSC**: Neural Stem Cells; **NURR1**: Nuclear Receptor-Related 1 Protein; **O4**: Oligodendrocyte Marker 4; **OLIG1**: Oligodendrocyte Transcription Factor 1; **OLIG2**: Oligodendrocyte Transcription Factor 2; **PDGFRα**: Platelet Derived Growth Factor Receptor alpha; **qPCR**: quantitative PCR; **RT-PCR**: Reverse Transcription-

Polymerase Chain Reaction; **S100B**: S100 calcium binding protein B; **scRNA-seq**: single-cell RNA sequencing **TH**: Tyrosine Hydroxylase; **TTX**: Tetrodotoxin; **VGLUT1**: Vesicular Glutamate Transporter 1; **VGLUT2**: Vesicular Glutamate Transporter 2; **VM**: Ventral Midbrain.

[1] Kim et al., 2021; the aim of this protocol is the enrichment of neural stem cells from human midbrain organoids that can be engrafted in a rodent PD model. It is the only 3D protocol that performed in vivo study. All data reported in Table 2b are related to the generation of in vitro midbrain-like organoids.

[2] Fiorenzano et al., (2021); compared midbrain-like organoid generation with and without spider-silk/laminin-511 scaffolding. Silk-scaffolded organoids showed superior outcomes; thus, all characterization data in Table 2b refer exclusively to those cultured on silk.

et al. (2017) highlighted batch-to-batch variability in midbrain marker expression, such as Engrailed-1 (EN1), even under standardized CHIR concentrations, occasionally resulting in hindbrain or diencephalic phenotype differentiation (Kirkeby et al., 2017). To mitigate this issue, Kim et al. (2021) introduced a biphasic WNT activation strategy comprising an initial low-dose CHIR phase mimicking early dose-dependent caudalization, followed by a subsequent high-dose "CHIR boost" to stabilize the ventral midbrain fate. This biphasic modulation more accurately recapitulated endogenous WNT1 signalling at the midbrain–hindbrain boundary, reducing off-target patterning and improving the consistency and quality of mDA neuron differentiation (T. W. Kim et al., 2021).

3.2. *Protocols for midbrain DA neurons differentiation in 3D cultures*

While 2D differentiation protocols have proven instrumental in establishing the molecular logic of mDA neuron specification, they remain limited in their capacity to recapitulate the cytoarchitectural complexity and network organization of the human brain. 3D culture systems, including organoids and assembloids, were therefore developed to better model ventral midbrain tissue architecture, cell–cell interactions, and long-term maturation of mDA neurons. In this context, several groups have established midbrain-like organoid protocols from human ESCs and iPSCs by adapting ventralization strategies originally optimized in 2D systems. These approaches aim to induce and maintain a ventral midbrain FP identity over extended culture periods, ultimately generating organoids enriched in functionally mature mDA neurons. Over the past decade, numerous protocols have been developed for generating midbrain-like organoids from human ESCs and iPSCs using ventralization strategies. However, achieving robust ventral midbrain authenticity requires precisely timed modulation of key developmental signaling pathways over extended culture periods, often spanning 100–120 days. Such prolonged culture frequently results in organoid heterogeneity, irregular morphology, and central necrosis, likely attributable to limited oxygen and nutrient diffusion. Eleven protocols were identified and systematically analyzed; their main features are summarized in Tables 1B and 2B. Tieng et al. (2014) were among the first authors to report the generation of midbrain-like organoids containing long-lived mDA neurons from ESCs and iPSCs. FP induction was achieved through dual-SMAD inhibition, followed by culture on engineered scaffolds composed of hydrophilic polytetrafluoroethylene membranes that enabled rapid generation of midbrain-like organoids containing TH-positive DA neurons within approximately three weeks (Tieng et al., 2014). Subsequent protocols achieved midbrain-like organoids via FP induction of iPSC-derived EBs maintained in suspension on orbital shakers (Jo et al., 2016; Qian et al., 2016). Jo et al. (2016) reported that approximately 22% of MAP2-positive neurons co-expressed TH by flow cytometry, and RNA-sequencing analysis revealed transcriptional profiles more closely resembling prenatal human midbrain than those obtained with 2D cultures (Jo et al., 2016). To reduce variability and improve mDA neuron yield, Monzel et al. (2017) combined Matrigel embedding with orbital shaking to generate midbrain-like organoids from iPSC-derived neural precursors following FP induction. This approach enriched for GIRK2/TH double-positive cells, indicative of A9-subtype mDA neurons, and flow cytometry of late-stage organoids demonstrated that approximately 64% of cells were triple-positive for TH, LMX1A, and FOXA2 (Monzel et al., 2017). Smits et al. (2019) developed an alternative approach using FP induction in ultra-low attachment round-bottom plates under static conditions, enabling efficient generation and expansion of midbrain FP precursors amenable to cryopreservation and subsequent organoid differentiation with improved efficiency (Smits et al., 2019). Building on the protocols of Monzel and Smits et al. (2019) optimized the method by increasing the initial number of FP progenitors, thereby enhancing organoid viability and reducing core necrosis. This protocol also yielded glial cells and multiple neuronal subtypes, with a predominance of A9-region mDA

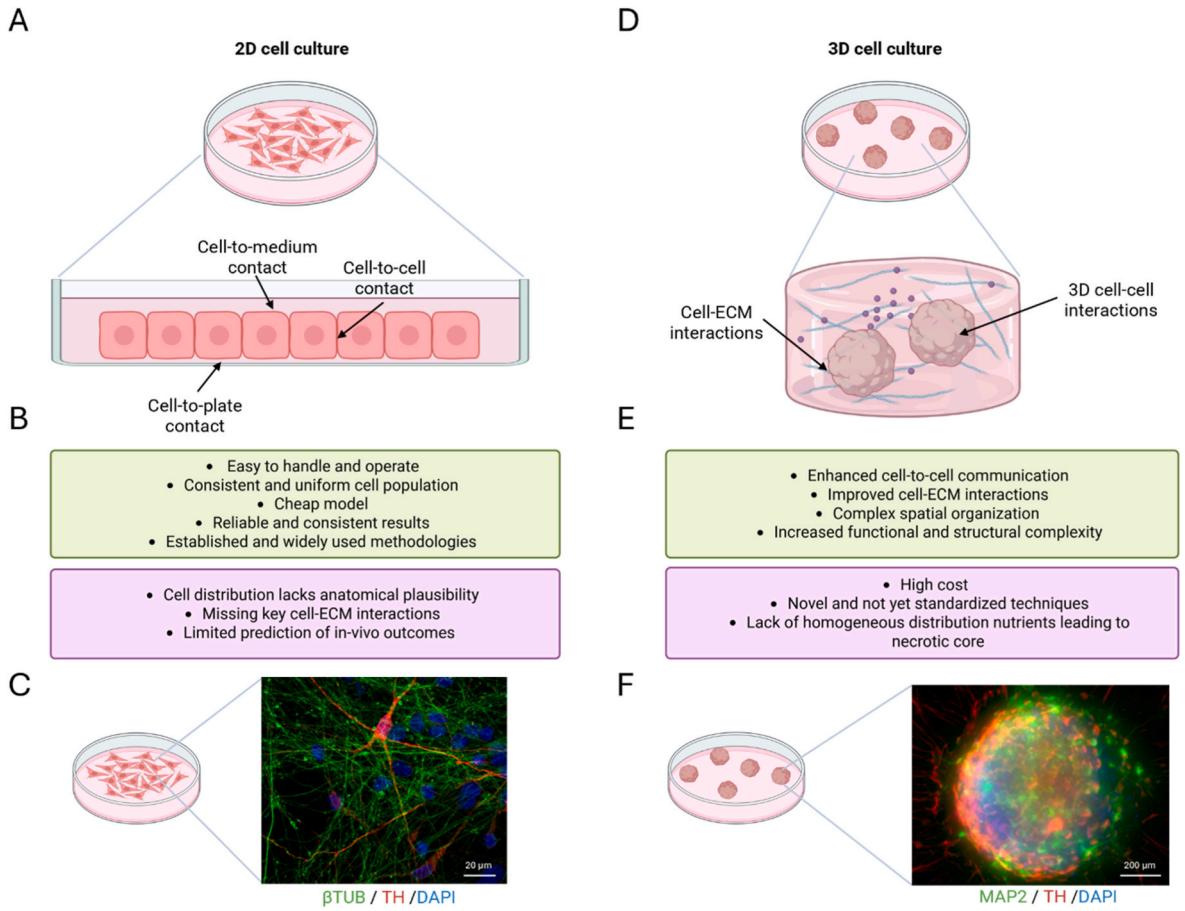

Fig. 1. Overview of the key features of 2-dimensional and 3-dimensional induced pluripotent stem cell-derived midbrain dopaminergic neuronal cultures. (A) 2D in vitro models. (B) Advantages and disadvantages of 2D in vitro models. (C) Representative immunofluorescence image of mDA neurons in 2D culture showing the expression of neuronal βIIITUB (green), DA neuron marker TH (red) and the nuclear staining with DAPI (blue). (D) 3D in vitro model. (E) Advantages and disadvantages of 3D in vitro models. (F) Representative immunofluorescence image of mDA neurons in 3D culture showing the expression of neuronal MAP2 (green), DA neuron marker TH (red) and nuclear staining with DAPI (blue) (Collo's Lab, unpublished data). **2D**: 2-Dimensional; **3D**: 3-Dimensional; **βTUB**: βIII-Tubulin; **DAPI**: 4′,6-diamidino-2-phenylindole; **ECM**: Extracellular Matrix; **MAP2**: Microtubule-Associated Protein 2; **TH**: Tyrosine Hydroxylase.

neurons (Nickels et al., 2020). Kim et al. (2021) generated midbrain-like organoids from iPSC-derived neural progenitors, achieving high yields of mDA neurons (45–50%) interspersed with astrocytes, along with improved synaptic maturity, functional activity, and expression of midbrain-specific markers (S. W. Kim et al., 2021). Sarrafha et al. (2021) developed a scalable protocol for large-scale production of uniform midbrain-like organoids with reduced heterogeneity. An optional CRISPR-mediated gene targeting step enabled the generation of TH-TdTomato reporter iPSC lines prior to organoid differentiation. Although the protocol required substantial medium volumes when employing up to nine spinner flasks per stirring plate, it could also be adapted to low-attachment 6-well plates under shaking conditions. Flow cytometry of dissociated organoids showed approximately 30% TH-positive neurons by day 30 of differentiation (Sarrafha et al., 2021). Fiorenzano et al. (2021) introduced a bioengineering approach to generate more homogeneous ventral midbrain organoids with reduced inter- and intra-organoid variability of several markers. Organoids were cultured on recombinant spider silk microfibers functionalized with full-length human laminin, forming a biocompatible 3D scaffold that promoted appropriate mDA neuron maturation. High proportions of TH-positive neurons (>60%) displayed the presence of neuromelanin in long-term cultures indicated advanced functional maturation (Fiorenzano et al., 2021). Subsequently, the same group published a simplified protocol for generating regionalized ventral midbrain organoids based on balanced modulation of patterning factors (Sozzi et al., 2022). iPSCs were first aggregated in conical wells to form EBs, which were then embedded in droplets of Matrigel, an heterogenous mixture of complex matrix proteins. This approach produced relatively immature mDA neurons within approximately 30 day of differentiation, and completely differentiated neurons, as evidenced by DAT and neuromelanin production, requiring 2–4 months in culture (Sozzi et al., 2022). Most recently, Reumann et al. (2023) introduced a protocol to generate ventral midbrain, striatal, and cortical organoids from iPSCs, which were subsequently fused into ventral midbrain – striatum –cortical assembloids using specialized polydimethylsiloxane embedding molds. Ventral midbrain patterning was achieved through dual-SMAD inhibition combined with Smoothened Agonist (SAG), striatal patterning via WNT Pathway Inhibitor 2 (IWP2) plus SAG, and cortical patterning using CHIR99021. The resulting assembloids contained functionally active DA projections that innervated both striatal and cortical compartments, providing a sophisticated in vitro model to investigate human basal ganglia - cortical circuitry (Reumann et al., 2023).

4. Authentication and characterization of midbrain DA neurons differentiated in 2D and 3D cultures

The protocols examined in this review employed these complementary analytical methods to authenticate the mDA neuron phenotype in both 2D monolayer and 3D organoid cultures. Techniques include Immunocytochemistry (ICC), Polymerase Chain Reaction (PCR), Real-Time Quantitative PCR (RT-qPCR), FACS, single-cell RNA sequencing (scRNA-seq), High-Performance Liquid Chromatography (HPLC) or

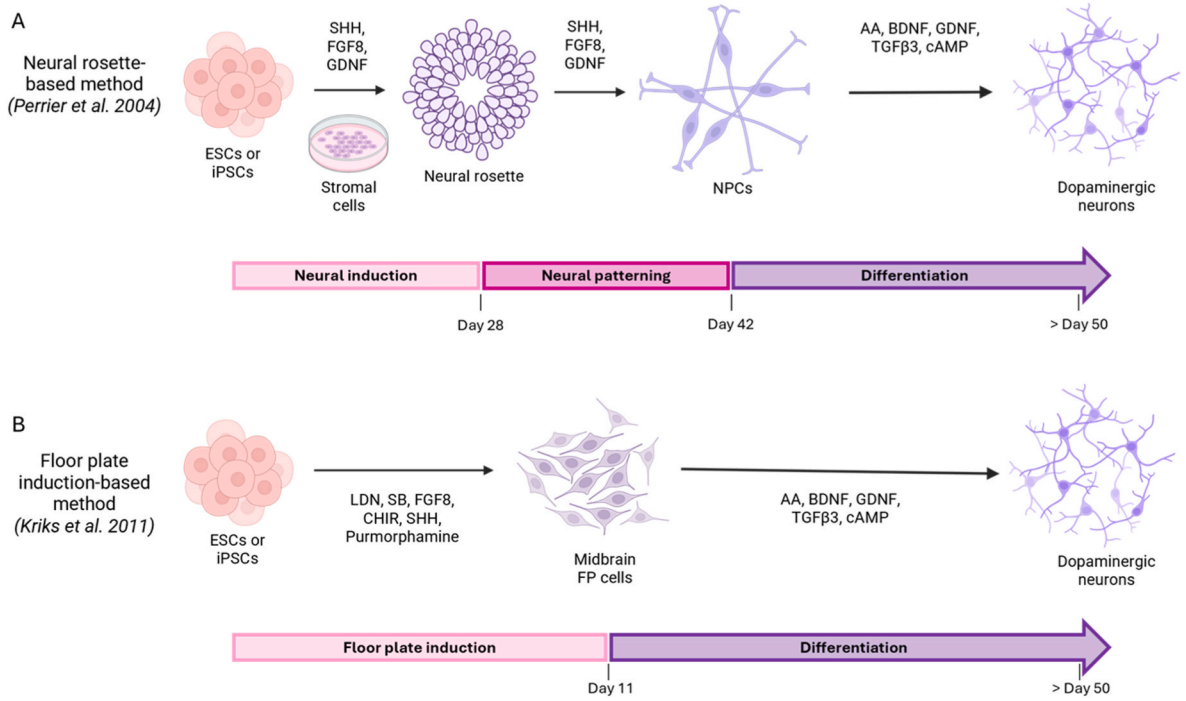

Fig. 2. Two approaches for deriving midbrain dopaminergic neurons from human embryonic stem cells and induced pluripotent stem cells. (A) Neural rosette-based differentiation (Perrier et al., 2004) (B) FP induction-based differentiation (Kriks et al., 2011). **AA**: Ascorbic Acid; **BDNF**: Brain-Derived Neurotrophic Factor; **cAMP**: Adenosine-3',5'-cyclic monophosphate; **CHIR**: CHIR99021; **ESCs**: Embryonic Stem Cells; **FP**: Floor Plate; **GDNF**: Glial Cell Line-Derived Neurotrophic Factor; **iPSCs**: Induced Pluripotent Stem Cells; **LDN**: LDN193189; **NPCs**: neural precursor cells; **SB**: SB431542; **SHH**; Sonic Hedgehog; **FGF8**: Fibroblast Growth Factor 8; **TGFβ3**: Transforming Growth Factor-beta 3.

Liquid Chromatography–Mass Spectrometry (LC-MS), electrophysiological recording, and in vivo transplantation studies (Table 2). These approaches were applied to ESC- and iPSC-derived mDA neurons at successive culture time points to monitor expression of neurodevelopmental markers involved in midbrain specification, such as EN1, Orthodenticle Homeobox 2 (OTX2), FOXA2, LMX1A, NURR1, and NGN2, as well as markers associated with acquisition of the mature mDA phenotype, including Vesicular Monoamine Transporter (VMAT), DAT, GIRK2, TH, and Aldehyde Dehydrogenase 1 Family, Member 1 (ALDH1A1). Gene level findings were corroborated at the protein level by ICC, with the proportion of TH-positive neurons serving as a key performance indicator of differentiation efficiency. Several groups further exploited scRNA-seq to resolve cellular heterogeneity and to delineate distinct mDA subpopulations within mixed cultures (Fiorenzano et al., 2021; Jo et al., 2016; S. W. Kim et al., 2021; T. W. Kim et al., 2021; Reumann et al., 2023; Sozzi et al., 2022). In midbrain-like organoid protocols, Fontana-Masson silver staining was used to detect neuromelanin, an insoluble black-brown granular pigment that accumulates selectively in substantia nigra pars compacta neurons in vivo (Fiorenzano et al., 2021; Jo et al., 2016; Monzel et al., 2017; Sozzi et al., 2022). The presence of neuromelanin provided strong evidence for regional midbrain identity and advanced maturation in long-term cultures. Electron microscopy, although employed less frequently, allowed high-resolution visualization of subcellular organelles and neuromelanin-like granules (Jo et al., 2016; Perrier et al., 2004). FACS was additionally applied to quantify or enrich cells expressing stage specific markers such as TH/TUJ1 and DAT (Fedele et al., 2017; Fiorenzano et al., 2021; Jo et al., 2016; Monzel et al., 2017; Sarrafha et al., 2021; Smits et al., 2019). Functional authenticity was assessed by measuring dopamine release and uptake. HPLC or LC-MS quantification of dopamine and its metabolites, including Homovanillic Acid (HVA) provided evidence of active presynaptic neurotransmission and by blockade of uptake using compounds selectively blocking DAT (Doi et al., 2014; Fedele et al., 2017; Jo et al., 2016; T. W. Kim et al., 2021; Kriks et al., 2011; Perrier et al., 2004; Tieng et al., 2014). Electrophysiological recordings, predominantly whole-cell patch-clamp in current-clamp mode, documented progressive functional maturation: early stage neurons exhibited low amplitude spontaneous firing and subthreshold oscillations characteristic of immature mDA cells (Doi et al., 2014; T. W. Kim et al., 2021; Kriks et al., 2011; Xi et al., 2012), whereas more mature neurons displayed robust tetrodotoxin sensitive sodium and potassium currents and the capacity to generate repetitive action potentials (Fiorenzano et al., 2021; Jo et al., 2016; Kirkeby et al., 2012; Perrier et al., 2004; Smits et al., 2019). GIRK and Hyperpolarization Activated Cyclic-Nucleotide-Gated (HCN) channels typical of mDA neurons contributed to the characteristic voltage sag response and pacemaker like spontaneous activity that enable tonic and burst firing patterns analogous to those recorded in substantia nigra neurons in vivo (Ballion et al., 2025; Fedele et al., 2017; Hartfield et al., 2014; T. W. Kim et al., 2021). In addition, mature cultures received heterologous synaptic inputs, exhibiting spontaneous excitatory postsynaptic currents mediated by glutamatergic transmission and forming synchronized network activity detectable with multi-electrode arrays (Kirkeby et al., 2012; Monzel et al., 2017; Smits et al., 2019; Tieng et al., 2014). Additional support for the authenticity of ESC- and iPSC-derived mDA neurons came from in vivo studies demonstrating successful engraftment and functional integration. For example, Fedele et al. (2017) transplanted neuronal precursors into the developing mouse embryonic brain and confirmed their capacity to integrate into host neural tissue (Fedele et al., 2017). Other groups evaluated therapeutic efficacy by grafting neural precursors cells or early-stage mDA neurons into the striatum of 6-Hydroxydopamine (6-OHDA)-lesioned rodents (S. W. Kim et al., 2021; T. W. Kim et al., 2021; Kriks et al., 2011; Sonntag et al., 2007; Sundberg et al., 2013; Swistowski et al., 2010), while alternative targets included the midbrain (Kirkeby et al., 2012) and putamen (Doi et al., 2014). Kriks et al. (2011) extended these findings to non-human primates by transplanting FP-derived mDA neurons into the caudate or putamen of 1-Methyl-4-Phenyl-1,2,3,6-Tetrahydropyridine

(MPTP)-lesioned rhesus monkeys, demonstrating robust graft survival and extensive fiber outgrowth at 30 days post-transplantation (Kriks et al., 2011). Mostly in 3D cultures, several protocols documented the expression of glial markers including S100 Calcium-Binding Protein B (S100B), Glial Fibrillary Acidic Protein (GFAP), S100 Calcium-Binding Protein A11 (S100A11), Aquaporin-4 (AQP4), Vimentin (VIM), Cyclic Nucleotide Phosphodiesterase (CNP), and Myelin Basic Protein (MBP), confirming the presence of astrocytes and oligodendrocytes that are critical for neuronal maturation, survival, and homeostasis (Fiorenzano et al., 2021; S. W. Kim et al., 2021; Monzel et al., 2017; Reumann et al., 2023; Sonntag et al., 2007). The emergence of glutamatergic, Gamma-Aminobutyric Acid (GABA)ergic, and serotonergic populations was also reported in both 2D and 3D cultures, reflecting the cellular diversity of the developing midbrain in vitro (Doi et al., 2014; Fiorenzano et al., 2021; S. W. Kim et al., 2021; Kriks et al., 2011; Nickels et al., 2020; Perrier et al., 2004; Qian et al., 2016; Reumann et al., 2023; Sundberg et al., 2013; Xi et al., 2012). Variability in mDA neuron yield across protocols is a fact, likely attributable to differences in differentiation procedures and maturation durations. Culture timelines ranged from relatively short paradigms of approximately 30 days characterize by stable TH expression but not by markers of maturations, to the 50-60 days generally used to achieve DAT expression and functional/electrophysiological similarity to mature mDA neurons (S. W. Kim et al., 2021; Nickels et al., 2020; Sundberg et al., 2013), extending to 70–120 days for more stable maturity and synaptic circuit functioning (Fedele et al., 2017; Fiorenzano et al., 2021; Kriks et al., 2011; Qian et al., 2016; Reumann et al., 2023; Smits et al., 2019) and with a further prolongation of differentiation to 200 and 240 days to investigate neuromelanin production and, eventually, toxic protein depositions (Sarrafha et al., 2021; Sozzi et al., 2022). Longer culture periods were generally associated with a higher variability among cultures and a higher maintenance workload for scientists.

5. iPSC-derived midbrain DA neurons for disease modeling and pharmacological studies

Several reviews focused on the application of iPSCs for disease modelling, specifically addressing disorders that involve mDA neuron pathology mainly regarding PD, but also some psychiatric disorders (Bose et al., 2022; Collo et al., 2018; Costamagna et al., 2021; Elvira et al., 2025; Slanzi et al., 2020). Here we discuss articles that exemplify the successfully implementation of the innovative protocols included in Tables 1 and 2 to develop disease models, aimed to provide example of the advancement of understanding of disease pathophysiology and of the implementation of pharmacological approaches. The selection of articles was based on their relevance in providing examples to support what proposed and did not claim any systematic intention to review the field.

5.1. Examples of 2D and 3D/organoid cultures for Parkinson disease modelling

The first attempt to model PD in vitro using a 2D culture paradigm was through the exposure to oxidative neurotoxin known to selectively disrupt DA system in vivo, such as 6-OHDA, MPTP, 1-Methyl-4-Phenylpyridinium (MPP^+), rotenone and paraquat, that were consistently implemented for in vivo studies (Bové and Perier, 2012; Dovonou et al., 2023). Using the medium conditioned by the stromal cell lines to induce DA phenotype development, Zeng et al. (2006) showed the possibility to damage human ESC-derived DA neurons with MPP^+ and rescue them with the Glial Cell Line-Derived Neurotrophic Factor (GDNF) (Zeng et al., 2006). Later, implementing the methods of Swistowski et al. (2010), Peng et al. (2013) were among the first to publish a medium-throughput screening to identified compounds that were neuroprotective vs. MPP^+ exposure by measuring cell viability, identifying, among others, amantadine, selegiline, nicotine, indomethacin, resveratrol, and N-acetyl cysteine. However, the complexity of using stromal cell lines, the lack of an extensive characterization of iPSCs derived neurons, the simple readout selected, and the low effects size might not fulfil the current standards, but it was first published example of screening applications for iPSC-derived DA neurons to model human PD pathogenesis in vitro (Peng et al., 2013). One of the latest examples of oxidative neurotoxins to model the key pathogenetic mechanisms of PD (and other brain disorders) can be seen in Jerber et al. (2020). This group differentiated 215 iPSC donated by healthy subjects in mDA neurons using the differentiation protocol of Kriks et al. (2011), developing a scale-up population approach for scRNA-seq, in the context of the HipSci project. Neurons in 2D cultures were harvested at different stages of differentiation, i.e., Day 11, 30 and 52 and Expression Quantitative Trait Loci (eQTL) were characterized either as control groups or after an oxidative stress produced by a single dose of rotenone (Jerber et al., 2020). Results indicated that 1284 genes co-localized with known neurological risk loci, but, disappointedly, only 1 with PD. The HipSci data were further analyzed using a two-step mendelian randomization design by integrating the Genome Wide Association Study (GWAS) for PD and the mDA neuron eQLT dataset of the control condition. The results indicated 10 risk genes with a potential casual role for PD pathogenesis, some of them already known (Dang et al., 2022). These attempts to model PD disease in vitro was importantly improved by Park et al. (2008), whose careful selection of donors for iPSCs with confirmed clinical and genetic diagnoses of familial PD cases, opened to the use of patient-specific iPSC-derived neurons in establishing in vitro models for PD (Park et al., 2008). Mitochondrial dysfunctions have been reported in PD familial cases of Parkin (PARK2), PTEN-Induced Kinase 1 (PINK1) (PARK6), DJ-1 (PARK7), Leucine-Rich Repeat Kinase 2 (LRRK2) (PARK8), and Coiled-Coil-Helix-Coiled-Coil-Helix Domain Containing 2 (CHCHD2) (PARK22)-linked, and several iPSCs were differentiated into mDA neurons to explore their functional genetic endophenotypes (Park et al., 2018). Using the inhibition of dual SMAD signalling inhibitor in combination with Noggin activity, CHIR99021 and purmorphamine (Chambers et al., 2009; Kriks et al., 2011) Yamaguchi et al. (2020) develop a standardized method to assess mitochondrial clearance, Reactive Oxygen Species (ROS) accumulation, and increasing apoptosis occurring in iPSC-derived DA neurons in 2D cultures from patients with familial PD carrying mutations in PARK6. These mutations were associated with a spontaneous and aberrant accumulation of mitochondria in the cytoplasm of DA neurons assessed at Day 10-17 in culture, on immature neurons. These authors screened 320 pre-selected compounds to identify drug candidates that ameliorated multiple phenotypes of iPSC-derived mDA neurons. Confirmatory functional analysis was performed in a Drosophila model. The iPSC-derived DA neurons screening identified 4 hits, i.e., tranylcypromine, flunarizine, bromocriptine, and MRS1220, in the 01-10 mM range. Only bromocriptine rescued the Drosophila larvae phenotype, suggesting therapeutic efficacy. Bromocriptine has been one of the first therapeutics available for PD since 1975, but currently it is less used due to its side effects (Boyd, 1995; Yamaguchi et al., 2020). Interesting results were obtained by Tabata et al. (2018) using PARK2 patient-specific, isogenic PARK2 null and PARK6 patient-specific iPSCs to generate DA neurons in 2D culture that spontaneously showed reduced complexity of neuronal processes and shorter neurites, and high sensitivity to rotenone-induced neurodegeneration, which was prevented by T-type calcium channel knockdown or pretreatment with antagonists, such as benidipine. To be noted, these studies relied on the protocol previously established in phenotyping the DA neurons, reducing the outcomes supporting of the authenticity of the mature phenotype to TH expression, therefore often studying immature phenotypes (e.g., 15-30 days of differentiation) that may not have acquired mesencephalic-like profile yet (e.g., expressing GIRK1, DAT/or neuromelanin) (Tabata et al., 2018). As a positive contribution, these articles factually support the multifactorial model of the disease based on concurring genetic liability, exposure to oxidative toxins, and rescue using pharmacological agents (Gao and Hong, 2011).

Accordingly, an exemplary article on in vitro dissection of the molecular mechanisms in PD, using iPSCs differentiated into DA neurons in 2D cultures differentiated with the Kriks et al. (2011) protocols, was carried out in the laboratory of Dimitri Krainc. iPSCs from sporadic PD patients, PD patients carrying a DJ-1 gene mutation, and control subjects were differentiated in DA neurons in 2D cultures. Studies were performed at 50, 75, 90 and 180 days of culture, showing a progressive increase of oxidized dopamine levels, increased deposition of neuromelanin, reduction of lysosome functioning and of Glucocerebrosidase (GCase) activity, leading to increase of α-synuclein aggregation, particularly evident in DJ-1 mutant mDA neurons. Intriguingly, treatment with the antioxidants N-acyl-cysteine and of the calcium channel inhibitor isradipine attenuated this pathogenetic profile (Burbulla et al., 2017). More recently, the 3D/midbrain-like organoid cultures containing DA neurons differentiated from human iPSCs were used for PD modelling (Costamagna et al., 2021; Elvira et al., 2025). Superiority of 3D vs. 2D cultures in authenticity for modelling PD disease was recognized as a common advantage, but evidence of proper pharmacological studies is limited to very few publications. Here we collected the articles that showed implementation of pharmacologic agents in PD disease models based on 3D/organoids described by the method listed in Table 2. Screening methodologies were developed to 3D/organoids generated from human iPSCs but not extensively implemented with chemical libraries (Renner et al., 2021). One model, defined BrainSpheres, was proposed for assessing mechanisms of developmental neuronal toxicology. These organoids displayed mixed aggregates of active DA, glutamatergic, GABAergic neurons, including glia and endothelial cells. At Day 28 of differentiation the immature organoids were exposed to 6-OHDA, MPTP, and MPP^{+}, and these neurotoxins selectively impaired the mDA neurons by altering maturity DA-related gene expression, causing selective DA neuron loss, increasing the organoid ROS production, and triggering mitochondrial dysfunction (Pamies et al., 2022). Focusing on authenticity, Monzel et al. (2017) tested the dopamine receptor D2-D3 antagonist quinpirole in midbrain organoids, showing reduced spontaneous pacemaker firing of the mDA neurons found interspaced in the 3D/organoid derived from healthy donors (Monzel et al., 2017). Regarding the use of genetics in PD disease modelling, isogenic 3D/midbrain-like organoids with PD-associated LRRK2 G2019S mutation was found recapitulate the 3D pathological hallmarks observed in PD patients with LRRK2 G2019S mutation, including reduce neurite length and reduced gene expression for NURR1, PITX3, EN1, TH, Microtubule Associated Protein Tau (MAPT) and a considerable increase of the thiol-oxidoreductase TXNIP found in the 3D/organoids, but not in 2D cultures (Kim et al., 2019). By developing a 3D/midbrain-like organoid system in a microfluidic platform, Bolognin et al. (2018) showed that iPSC-derived mDA neurons carrying the LRRK2-G2019S mutation displayed neurite branching deficits and mitochondrial abnormalities. More importantly, treatment with the selective LRRK2 inhibitor Inh2 rescued these mDA neurons from spontaneous defective development, normalizing their morphology and functions (Bolognin et al., 2018).Technological advancements in improving the detection of pharmacological effects were recently proposed. An et al. (2024) developed a 3D concave electrode patterned with a mesoporous Au nanodot for the detection of electrochemical signals of dopamine levels obtained from midbrain-like organoids differentiated for several months from iPSCs of donors with LRKK2 and PRKN mutation or from healthy volunteers. Pharmacological validation was obtained with levodopa, the main treatment for PD, showing a dose-dependent increase of the dopamine electrochemical signals (An et al., 2024). In another study, an optogenetics-assisted α-synuclein aggregation induction system was developed in iPSC-derived 3D/midbrain-like organoids with the aim to accelerate the occurrence of DA neuron specific pathology by amplifying the α-synuclein aggregate formation, so to allow efficient drug screening in midbrain-like organoids generated using the protocol of Jo et al. (2016). The study identified a novel Phosphoinositide 3-Kinase (PI3K) inhibitor (BAG956) that was able to promote autophagic clearance of α-synuclein aggregates, pointing again on a role for the Mammalian Target of Rapamycin (mTOR) pathways (Kim et al., 2023).

5.2. *Examples of 2D and 3D/organoid cultures for psychiatric disease modeling*

iPSC-derived mDA neurons were used to model psychiatric disorders known to have dysfunctional mesocortical and/or mesolimbic DA system. Some reviews addressed the various aspects of iPSC-derived neurons methodologies in psychiatric research (Collo et al., 2020; Dutan Polit et al., 2023; Quadrato et al., 2016; Rossetti et al., 2019; Soliman et al., 2017), showing that, except for very early studies (Hartley et al., 2015; Robicsek et al., 2013), the mDA phenotype was not extensively studied, also due to a preference given to telencephalic glutamatergic or GABAergic neurons (Soliman et al., 2017). Here we reviewed the articles available on iPSCs derived mDA neuron for psychiatric research. Using a dual-SMAD inhibition approach, Robicsek et al. (2013) found mitochondrial impairment in relatively immature mDA neurons differentiated from iPSCs from patients with schizophrenia (Robicsek et al., 2013). This protocol was modified by Hartley et al. (2015) showing electrophysiological features compatible with mature DA neurons, whose firing was attenuated by quinpirole (Hartley et al., 2015). More recently, Hartmann et al. (2025) reported observation of co-cultures of mDA neurons and glutamatergic neurons differentiated from iPSCs of patients with schizophrenia established as in vitro model design to mimic prefrontal lobe interactions. Since the differentiation protocol to obtain the mDA phenotype was through forced induction via Achaete-Scute Complex Homologue 1 (ASCL1)/LMX1B/NURR1 transcription factors, confirmatory studies using dual SMAD inhibition differentiation for regular iPSCs are awaited (Hartmann et al., 2025). In another study, a mendelian randomization design was used to integrate GWAS of schizophrenia (74,776 cases and 101,023 controls) to the DA neuron eQLT data from the 215 iPSCs derived DA neurons form healthy volunteers profiled with scRNA-seq in the HiSci project, resulting in 2 high probability causal genes DDHD Domain-Containing Protein 2 (DDHD2) and Polypeptide N-Acetylgalactosaminyltransferase 10 (GALNT10) (Dang et al., 2023), awaiting further confirmation.

For Mood Disorders, no publication showing iPSCs from patients differentiated in mDA neurons as disease models for pharmacological studies was found. However, one in vitro endocrine model of the hypercortisolemia that characterize Major Depressive Disorder was recently published on mDA neurons differentiated using the Kriks et al. (2011) modified by Fedele et al. (2017), showing that impairment of dendritic arborization produced by cortisol can be rescued by the antidepressant ketamine at low doses, via a Brain-Derived Neurotrophic Factor (BDNF)/mTOR mediated pathway, highlighting the model potential for studying antidepressant drugs acting through neuronal plasticity (Cavalleri et al., 2024). Regarding Attentional Deficit Hyperactivity Disorder (ADHD), Palladino et al. (2020) studied iPSCs differentiated in DA neurons from ADHD patients carrying Copy Number Variations (CNVs) in the PARK2 gene using the 2D differentiation protocol of Kriks et al. (2011) with modifications. Reduced PARK2 expression, ATP production, and basal oxygen consumption rate were reported in the mDA neurons of ADHD patients carrying PARK2 CNVs deletion or duplication, suggesting a possible pathological relevance (Palladino et al., 2020). Accordingly, neuronal precursor cells from ADHD patients proliferated significantly less than controls, suggesting developmental delays and lower cellular metabolic rate that may affect the maturation of DA neurons (Yde Ohki et al., 2023). Interestingly, in spite extensive investigations of Autism Spectrum Disorder powered by 2D and 3D iPSCs derived neurons were dedicated to study their excitatory-inhibitory makeup (Kilpatrick et al., 2023; Pintacuda et al., 2021), we could not find any article properly addressing their DA phenotype. Finally, in a very interesting study on Substance Use Disorders, Sheng et al. (2016) obtained DA neurons from iPSCs derived from 10 opioid-dependent and 10 control subjects carrying different 3'

Variable Number Tandem Repeat Polymorphism (3′ VNTR) in the DAT gene (SLC6A3), using the Kirks et al. (2011) protocol. Results showed that the 3′ VNTR polymorphism changed the DAT expression levels differently in opioid-dependent subjects vs. controls, and that 5-day exposure to 0.6 mM valproic acid (from differentiation Day 23 to 28) produced a strong increase of DAT expression in all DA neurons with the 9/9 genotype and an of dopamine receptor D2 expression and of dopamine release only in the opioid-dependent subjects (Sheng et al., 2016).

6. Conclusions

The establishment of robust and standardized differentiation protocols for developing viable iPSC-derived mDA neurons and the application of a consensus authenticity pipelines represents a critical step towards the translation from cellular neuroscience to clinical implementation under the framework of the personalized medicine paradigm. Comparative analysis demonstrates that while 2D systems remain important for disease modeling and medium-throughput screening, 3D/organoid-offer higher physiological relevance, cellular diversity, and connectivity complexity, that, associated to recent technological improvement, would allow soon more standardized settings for screening and pharmacological tests. Among the various approaches reviewed in this study, the protocols based on dual-SMAD inhibition and FP induction can be considered as the most reproducible and efficient procedure for generating functional iPSC-derived mDA neurons. The improvement in the outcome variability was obtained by using the biphasic WNT activation strategy (T. W. Kim et al., 2021) and by implementing a pre-differentiation step of neuronal precursor expansion (Fedele et al., 2017), bringing the 2D approach to a very good level of reliability. Moreover, improvements of xeno-free media capable of sustaining extended differentiation periods, and the availability of a comprehensive multimodal validation tools (i.e., morphological, molecular, electrophysiological, and functional assays) are at the basis to ensure both authenticity and experimental reproducibility. The recent and ongoing development of various 3D bioengineered systems including midbrain-like organoids and assembloids has proposed several protocols, whose performance is still under evaluation. It is maintained that their development will surely advance the field by enabling the reconstruction of DA systems and more accurate modeling of specific aspects of neurodegenerative and psychiatric disorders, hopefully providing an actionable translational paradigm for personalized medicine.

Credit author statement

Conceptualization: GSM, JB, EMP, GC.
Formal analysis: GSM, JB, EMP, GC.
Writing – original draft: GSM, JB.
Writing – review and editing: EMP, GC.
Supervision: GC.
Funding acquisition: GC.

Author disclosure

This work was supported by Grant from ex 60% University of Brescia to Ginetta Collo. The funding source has not involvement in the study design, in the collection, analysis and interpretation of data, in writing and submitting the article for publication.

Declaration of competing interest

The authors declare the following financial interests/personal relationships which may be considered as potential competing interests:

G.C. is member of the editorial board of Neuroscience Applied as peer reviewer. Given her role, had no involvement in the peer review of this article and had no access to information regarding its peer review. Full responsibility for the editorial process for this article was delegated to another journal editor. If there are other authors, they declare that they have no known competing financial interests or personal relationships that could have appeared to influence the work reported in this paper. Emilio Merlo Pich is consultant for Novavido, G-Factor, MgShell and Apllied Cognition, the present work was carried out as in-kind.

Abbreviations

2D	2-Dimensional
3′ VNTR	Variable Number Tandem Repeat Polymorphism
3D	3-Dimensional
6-OHDA	6-Hydroxydopamine
ADHD	Attentional Deficit Hyperactivity Disorder
ALDH1A1	Aldehyde Dehydrogenase 1 Family, Member 1
AQP4	Aquaporin 4
ASCL1	Achaete-Scute Complex Homologue 1
BDNF	Brain-Derived Neurotrophic Factor
BMP	Bone Morphogenetic Protein
CHCHD2	Coiled-Coil-Helix-Coiled-Coil-Helix Domain Containing 2
CNP	Cyclic Nucleotide Phosphodiesterase
CNVs	Copy Number Variations
DA	Dopaminergic
DAT	Dopamine Transporter
DDHD2	Ddhd Domain-Containing Protein 2
EBs	Embryoid Bodies
EN1	Engrailed-1
eQTL	Expression Quantitative Trait Loci
ESCs	Embryonic Stem Cells
FACS	Fluorescence-Activeted Cell Sorting
FGF8	Fibroblast Growth Factor 8
FOXA2	Forkhead Box A2
FP	Floor Plate
GABA	Gamma-Aminobutyric Acid
GCase	Glucocerebrosidase
GFAP	Glial Fibrillary Acidic Protein
GIRK2	G-Protein–Regulated Inward-Rectifier Potassium Channel 2

(*continued on next page*)

(*continued*)

GLANT10	Polypeptide N-Acetylgalactosaminyltransferase 10
GSK3β	Glycogen Synthase Kinase 3 Beta
GWAS	Genome Wide Association Study
HCN	Hyperpolarization Activated Cyclic-Nucleotide-Gated
HPLC	High-Pressure Liquid Chromatography
HVA	Homovanillic Acid
ICC	Immunocytochemistry
iDA	Induced Dopaminergic
iPSCs	Induced Pluripotent Stem Cells
IWP2	Wnt Pathway Inhibitor 2
LC-MS	Liquid Chromatography–Mass Spectrometry
LMX1A	LIM Homeobox Transcription Factor 1-Alpha
LMX1B	LIM Homeobox Transcription Factor 1-Beta
LRRK2	Leucine-Rich Repeat Kinase 2
MAPT	Microtubule Associated Protein Tau
MBP	Myelin Basic Protein
mDA	Midbrain Dopaminergic
MPP^+	1-Methyl-4-Phenylpyridinium
MPTP	1-Methyl-4-Phenyl-1,2,3,6-Tetrahydropyridine
MSX1	Msh Homeobox 1
mTOR	Mammalian Target Of Rapamycin
NGN	Neurogenin
NURR1	Nuclear Receptor-Related 1 Protein
OTX2	Orthodenticle Homeobox 2
PCR	Polymerase Chain Reaction
PD	Parkinson's Disease
PI3K	Phosphoinositide 3-Kinase
PINK1	PTEN-Induced Kinase 1
PITX3	Pituitary Homeobox 3
ROS	Reactive Oxygen Species
RT-qPCR	Real-Time Quantitative PCR
S100A11	S100 Calcium-Binding Protein A11
S100B	S100 Calcium-Binding Protein B
SAG	Smoothened Agonist
scRNA-seq	Single-Cell RNA Sequencing
SHH	Sonic Hedgehog Protein
TGFβ	Transforming Growth Factor-beta
TH	Tyrosine Hydroxylase
VIM	Vimentin
VMAT	Vesicular Monoamine Transporter

References

An, J., Shin, M., Beak, G., Yoon, J., Kim, S., Cho, H.Y., Choi, J.W., 2024. Drug Evaluation of Parkinson's Disease Patient-Derived Midbrain Organoids Using Mesoporous Au Nanodot-Patterned 3D Concave Electrode. ACS Sens. 9 (7), 3573–3580. https://doi.org/10.1021/ACSSENSORS.4C00476.

Arenas, E., 2014. Wnt signaling in midbrain dopaminergic neuron development and regenerative medicine for Parkinson's disease. J. Mol. Cell Biol. 6 (1), 42–53. https://doi.org/10.1093/JMCB/MJU001.

Arenas, E., Denham, M., Villaescusa, J.C., 2015. How to make a midbrain dopaminergic neuron. Development (Cambridge, U. K.) 142 (11), 1918–1936. https://doi.org/10.1242/DEV.097394.

Ballion, B., Bonnet, M.L., Brot, S., Gaillard, A., 2025. Electrophysiological characterisation of intranigral-grafted hiPSC-derived dopaminergic neurons in a mouse model of Parkinson's disease. Stem Cell Res. Ther. 16 (1), 232. https://doi.org/10.1186/S13287-025-04344-Z, 2025 16:1.

Birtele, M., Storm, P., Sharma, Y., Kajtez, J., Wahlestedt, J.N., Sozzi, E., Nilsson, F., Stott, S., He, X.L., Mattsson, B., Ottosson, D.R., Barker, R.A., Fiorenzano, A., Parmar, M., 2022. Single-cell transcriptional and functional analysis of dopaminergic neurons in organoid-like cultures derived from human fetal midbrain. Development: For Advances in Developmental Biology and Stem Cells 149 (23), dev200504. https://doi.org/10.1242/DEV.200504.

Bloem, B.R., Okun, M.S., Klein, C., 2021. Parkinson's disease. Lancet 397 (10291), 2284–2303. https://doi.org/10.1016/S0140-6736(21)00218-X.

Bolognin, S., Fossépré, M., Qing, X., Jarazo, J., Ščančar, J., Moreno, E.L., Nickels, S.L., Wasner, K., Ouzren, N., Walter, J., Grünewald, A., Glaab, E., Salamanca, L., Fleming, R.M.T., Antony, P.M.A., Schwamborn, J.C., 2018. 3D cultures of Parkinson's disease-specific dopaminergic neurons for high content phenotyping and drug testing. Adv. Sci. (Weinh.) 6 (1). https://doi.org/10.1002/ADVS.201800927.

Bose, A., Petsko, G.A., Studer, L., 2022. Induced pluripotent stem cells: a tool for modeling Parkinson's disease. Trends Neurosci. 45 (8), 608–620. https://doi.org/10.1016/j.tins.2022.05.001.

Bové, J., Perier, C., 2012. Neurotoxin-based models of Parkinson's disease. Neuroscience 211, 51–76. https://doi.org/10.1016/j.neuroscience.2011.10.057.

Boyd, A., 1995. Bromocriptine and psychosis: a literature review. Psychiatr. Q. 66 (1), 87–95. https://doi.org/10.1007/BF02238717.

Burbulla, L.F., Song, P., Mazzulli, J.R., Zampese, E., Wong, Y.C., Jeon, S., Santos, D.P., Blanz, J., Obermaier, C.D., Strojny, C., Savas, J.N., Kiskinis, E., Zhuang, X., Krüger, R., Surmeier, D.J., Krainc, D., 2017. Dopamine oxidation mediates mitochondrial and lysosomal dysfunction in Parkinson's disease. Science (New York, N.Y.) 357 (6357), 1255–1261. https://doi.org/10.1126/SCIENCE.AAM9080.

Caiazzo, M., Dell'Anno, M.T., Dvoretskova, E., Lazarevic, D., Taverna, S., Leo, D., Sotnikova, T.D., Menegon, A., Roncaglia, P., Colciago, G., Russo, G., Carninci, P., Pezzoli, G., Gainetdinov, R.R., Gustincich, S., Dityatev, A., Broccoli, V., 2011. Direct generation of functional dopaminergic neurons from mouse and human fibroblasts. Nature 476 (7359), 224–227. https://doi.org/10.1038/NATURE10284.

Carter, J.L., Halmai, J.A.N.M., Fink, K.D., 2020. The iNs and outs of direct reprogramming to induced neurons. Frontiers in Genome Editing 2. https://doi.org/10.3389/FGEED.2020.00007.

Cavalleri, L., Dassieni, I., Marcotto, G.S., Zoli, M., Merlo Pich, E., Collo, G., 2024. Cortisol-dependent impairment of dendrite plasticity in human dopaminergic neurons derived from hiPSCs is restored by ketamine: relevance for major depressive disorders. Neuroscience Applied 3, 104049. https://doi.org/10.1016/J.NSA.2024.104049.

Chambers, S.M., Fasano, C.A., Papapetrou, E.P., Tomishima, M., Sadelain, M., Studer, L., 2009. Highly efficient neural conversion of human ES and iPS cells by dual inhibition of SMAD signaling. Nat. Biotechnol. 27 (3), 275–280. https://doi.org/10.1038/nbt.1529.

Chung, S., Leung, A., Han, B.S., Chang, M.Y., Moon, J. Il, Kim, C.H., Hong, S., Pruszak, J., Isacson, O., Kim, K.S., 2009. Wnt1-lmx1a forms a novel autoregulatory loop and controls midbrain dopaminergic differentiation synergistically with the SHH-FoxA2 pathway. Cell Stem Cell 5 (6), 646–658. https://doi.org/10.1016/j.stem.2009.09.015.

Collo, G., Mucci, A., Giordano, G.M., Merlo Pich, E., Galderisi, S., 2020. Negative symptoms of schizophrenia and dopaminergic transmission: Translational models and perspectives opened by iPSC techniques. Front. Neurosci. 14. https://doi.org/10.3389/FNINS.2020.00632.

Collo, G., Cavalleri, L., Bono, F., Mora, C., Fedele, S., Invernizzi, R.W., Gennarelli, M., Piovani, G., Kunath, T., Millan, M.J., Merlo Pich, E., Spano, P., 2018. Ropinirole and pramipexole promote structural plasticity in human iPSC-Derived dopaminergic neurons via BDNF and mTOR signaling. Neural Plast. 2018. https://doi.org/10.1155/2018/4196961.

Comella-Bolla, A., Orlandi, J.G., Miguez, A., Straccia, M., García-Bravo, M., Bombau, G., Galofré, M., Sanders, P., Carrere, J., Segovia, J.C., Blasi, J., Allen, N.D., Alberch, J., Soriano, J., Canals, J.M., 2020. Human pluripotent stem cell-derived neurons are functionally mature in vitro and integrate into the mouse striatum following transplantation. Mol. Neurobiol. 57 (6), 2766–2798. https://doi.org/10.1007/S12035-020-01907-4.

Cooper, O., Hargus, G., Deleidi, M., Blak, A., Osborn, T., Marlow, E., Lee, K., Levy, A., Perez-Torres, E., Yow, A., Isacson, O., 2010. Differentiation of human ES and Parkinson's disease iPS cells into ventral midbrain dopaminergic neurons requires a high activity form of SHH, FGF8a and specific regionalization by retinoic acid. Mol. Cell. Neurosci. 45 (3), 258–266. https://doi.org/10.1016/j.mcn.2010.06.017.

Costamagna, G., Comi, G. Pietro, Corti, S., 2021. Advancing drug discovery for neurological disorders using iPSC-Derived neural organoids. Int. J. Mol. Sci. 22 (5), 1–21. https://doi.org/10.3390/IJMS22052659.

Dang, X., Liu, J., Zhang, Z., Luo, X.J., 2023. Mendelian randomization study using dopaminergic neuron-specific eQTL identifies novel risk genes for schizophrenia. Mol. Neurobiol. 60 (3), 1537–1546. https://doi.org/10.1007/S12035-022-03160-3.

Dang, X., Zhang, Z., Luo, X.J., 2022. Mendelian randomization study using dopaminergic neuron-specific eQTL nominates potential causal genes for parkinson's disease. Mov. Disord. : Official Journal of the Movement Disorder Society 37 (12), 2451–2456. https://doi.org/10.1002/MDS.29239.

Doi, D., Samata, B., Katsukawa, M., Kikuchi, T., Morizane, A., Ono, Y., Sekiguchi, K., Nakagawa, M., Parmar, M., Takahashi, J., 2014. Isolation of human induced pluripotent stem cell-derived dopaminergic progenitors by cell sorting for successful transplantation. Stem Cell Rep. 2 (3), 337–350. https://doi.org/10.1016/j.stemcr.2014.01.013.

Dong-Chen, X., Yong, C., Yang, X., Chen-Yu, S.T., Li-Hua, P., 2023. Signaling pathways in Parkinson's disease: molecular mechanisms and therapeutic interventions. Signal Transduct. Targeted Ther. 8 (1), 73. https://doi.org/10.1038/s41392-023-01353-3, 2023 8:1.

Dovonou, A., Bolduc, C., Soto Linan, V., Gora, C., Peralta, M.R., Lévesque, M., 2023. Animal models of Parkinson's disease: bridging the gap between disease hallmarks and research questions. Transl. Neurodegener. 12 (1), 36. https://doi.org/10.1186/S40035-023-00368-8, 2023 12:1.

Dutan Polit, L., Eidhof, I., McNeill, R.V., Warre-Cornish, K.M., Yde Ohki, C.M., Walter, N. M., Sala, C., Verpelli, C., Radtke, F., Galderisi, S., Mucci, A., Collo, G., Edenhofer, F., Castrén, M.L., Réthelyi, J.M., Ejlersen, M., Hohmann, S.S., Ilieva, M.S., Lukjanska, R., et al., 2023. Recommendations, guidelines, and best practice for the use of human induced pluripotent stem cells for neuropharmacological studies of neuropsychiatric disorders. Neuroscience Applied 2, 101125. https://doi.org/10.1016/J.NSA.2023.101125.

Elvira, R., Tan, E.K., Zhou, Z.D., 2025. Three-dimensional midbrain organoids: a next-generation tool for Parkinson's disease modelling and drug discovery. Stem Cell Res. Ther. 16 (1), 502. https://doi.org/10.1186/S13287-025-04660-4, 2025 16:1.

Fedele, S., Collo, G., Behr, K., Bischofberger, J., Müller, S., Kunath, T., Christensen, K., Gündner, A.L., Graf, M., Jagasia, R., Taylor, V., 2017. Expansion of human midbrain floor plate progenitors from induced pluripotent stem cells increases dopaminergic neuron differentiation potential. Sci. Rep. 7 (1). https://doi.org/10.1038/s41598-017-05633-1.

Fiorenzano, A., Sozzi, E., Birtele, M., Kajtez, J., Giacomoni, J., Nilsson, F., Bruzelius, A., Sharma, Y., Zhang, Y., Mattsson, B., Emnéus, J., Ottosson, D.R., Storm, P., Parmar, M., 2021. Single-cell transcriptomics captures features of human midbrain development and dopamine neuron diversity in brain organoids. Nat. Commun. 12 (1). https://doi.org/10.1038/s41467-021-27464-5.

Gao, H.M., Hong, J.S., 2011. Gene-environment interactions: key to unraveling the mystery of Parkinson's disease. Prog. Neurobiol. 94 (1), 1–19. https://doi.org/10.1016/J.PNEUROBIO.2011.03.005.

Grace, A.A., 2016. Dysregulation of the dopamine system in the pathophysiology of schizophrenia and depression. Nat. Rev. Neurosci. 17 (8), 524–532. https://doi.org/10.1038/NRN.2016.57.

Hartfield, E.M., Yamasaki-Mann, M., Ribeiro Fernandes, H.J., Vowles, J., James, W.S., Cowley, S.A., Wade-Martins, R., 2014. Physiological characterisation of human iPS-Derived dopaminergic neurons. PLoS One 9 (2), e87388. https://doi.org/10.1371/JOURNAL.PONE.0087388.

Hartley, B.J., Tran, N., Ladran, I., Reggio, K., Brennand, K.J., 2015. Dopaminergic differentiation of schizophrenia hiPSCs. Mol. Psychiatr. 20 (5), 549–550. https://doi.org/10.1038/MP.2014.194.

Hartmann, S.M., Pizarro Garcia, P., Heider, J., Vogel, S., Wüstner, L.S., Wüst, R., Fallgatter, A.J., Volkmer, H., 2025. A co-culture model of dopaminergic and glutamatergic neurons derived from patients with idiopathic schizophrenia reveals a hypodopaminergic phenotype. Mol. Psychiatr. 1–14. https://doi.org/10.1038/s41380-025-03384-4, 2025.

Hegarty, S.V., Sullivan, A.M., O'Keeffe, G.W., 2013. Midbrain dopaminergic neurons: a review of the molecular circuitry that regulates their development. Dev. Biol. 379 (2), 123–138. https://doi.org/10.1016/j.ydbio.2013.04.014.

Jerber, J., Seaton, D., Cuomo, A., Kumasaka, N., Haldane, J., Steer, J., Patel, M., Pearce, D., Andersson, M., Bonder, M., Mountjoy, E., Ghoussaini, M., Lancaster, M., Consortium, H., Marioni, J., Merkle, F., Stegle, O., Gaffney, D., 2020. Population-scale single-cell RNA-seq profiling across dopaminergic neuron differentiation. bioRxiv. https://doi.org/10.1101/2020.05.21.103820, 2020.05.21.103820.

Jo, J., Xiao, Y., Sun, A.X., Cukuroglu, E., Tran, H.D., Göke, J., Tan, Z.Y., Saw, T.Y., Tan, C.P., Lokman, H., Lee, Y., Kim, D., Ko, H.S., Kim, S.O., Park, J.H., Cho, N.J., Hyde, T.M., Kleinman, J.E., Shin, J.H., et al., 2016. Midbrain-like organoids from human pluripotent stem cells contain functional dopaminergic and neuromelanin-producing neurons. Cell Stem Cell 19 (2), 248–257. https://doi.org/10.1016/j.stem.2016.07.005.

Kilpatrick, S., Irwin, C., Singh, K.K., 2023. Human pluripotent stem cell (hPSC) and organoid models of autism: opportunities and limitations. Transl. Psychiatry 13 (1), 217. https://doi.org/10.1038/s41398-023-02510-6, 2023 13:1.

Kim, H., Park, H.J., Choi, H., Chang, Y., Park, H., Shin, J., Kim, J., Lengner, C.J., Lee, Y. K., Kim, J., 2019. Modeling G2019S-LRRK2 sporadic parkinson's disease in 3D midbrain organoids. Stem Cell Rep. 12 (3), 518–531. https://doi.org/10.1016/j.stemcr.2019.01.020.

Kim, J., Koo, B.K., Knoblich, J.A., 2020. Human organoids: model systems for human biology and medicine. Nat. Rev. Mol. Cell Biol. 21 (10), 571–584. https://doi.org/10.1038/s41580-020-0259-3, 2020 21:10.

Kim, M.S., Ra, E.A., Kweon, S.H., Seo, B.A., Ko, H.S., Oh, Y., Lee, G., 2023. Advanced human iPSC-based preclinical model for Parkinson's disease with optogenetic alpha-synuclein aggregation. Cell Stem Cell 30 (7), 973–986.e11. https://doi.org/10.1016/j.stem.2023.05.015.

Kim, S.W., Woo, H.J., Kim, E.H., Kim, H.S., Suh, H.N., Kim, S. hyun, Song, J.J., Wulansari, N., Kang, M., Choi, S.Y., Choi, S.J., Jang, W.H., Lee, J., Kim, K.H., Lee, W., Kim, S.H., Yang, J., Kyung, J., Lee, H.S., et al., 2021. Neural stem cells derived from human midbrain organoids as a stable source for treating Parkinson's disease: midbrain organoid-NSCs (Og-NSC) as a stable source for PD treatment. Prog. Neurobiol. 204. https://doi.org/10.1016/j.pneurobio.2021.102086.

Kim, T.W., Piao, J., Koo, S.Y., Kriks, S., Chung, S.Y., Betel, D., Socci, N.D., Choi, S.J., Zabierowski, S., Dubose, B.N., Hill, E.J., Mosharov, E.V., Irion, S., Tomishima, M.J., Tabar, V., Studer, L., 2021. Biphasic activation of WNT signaling facilitates the derivation of midbrain dopamine neurons from hESCs for translational use. Cell Stem Cell 28 (2), 343–355.e5. https://doi.org/10.1016/j.stem.2021.01.005.

Kirkeby, A., Grealish, S., Wolf, D.A., Nelander, J., Wood, J., Lundblad, M., Lindvall, O., Parmar, M., 2012. Generation of regionally specified neural progenitors and functional neurons from human embryonic stem cells under defined conditions. Cell Rep. 1 (6), 703–714. https://doi.org/10.1016/j.celrep.2012.04.009.

Kirkeby, A., Nolbrant, S., Tiklova, K., Heuer, A., Kee, N., Cardoso, T., Ottosson, D.R., Lelos, M.J., Rifes, P., Dunnett, S.B., Grealish, S., Perlmann, T., Parmar, M., 2017. Predictive markers guide differentiation to improve graft outcome in clinical translation of hESC-Based therapy for parkinson's disease. Cell Stem Cell 20 (1), 135–148. https://doi.org/10.1016/j.stem.2016.09.004.

Klein, M.O., Battagello, D.S., Cardoso, A.R., Hauser, D.N., Bittencourt, J.C., Correa, R.G., 2019. Dopamine: functions, signaling, and association with neurological diseases. Cell. Mol. Neurobiol. 39 (1), 31–59. https://doi.org/10.1007/S10571-018-0632-3.

Kriks, S., Shim, J.W., Piao, J., Ganat, Y.M., Wakeman, D.R., Xie, Z., Carrillo-Reid, L., Auyeung, G., Antonacci, C., Buch, A., Yang, L., Beal, M.F., Surmeier, D.J., Kordower, J.H., Tabar, V., Studer, L., 2011. Dopamine neurons derived from human ES cells efficiently engraft in animal models of Parkinson's disease. Nature 480 (7378), 547–551. https://doi.org/10.1038/nature10648.

La Manno, G., Gyllborg, D., Codeluppi, S., Nishimura, K., Salto, C., Zeisel, A., Borm, L.E., Stott, S.R.W., Toledo, E.M., Villaescusa, J.C., Lönnerberg, P., Ryge, J., Barker, R.A., Arenas, E., Linnarsson, S., 2016. Molecular diversity of midbrain development in mouse, human, and stem cells. Cell 167 (2), 566–580.e19. https://doi.org/10.1016/j.cell.2016.09.027.

Marton, R.M., Ioannidis, J.P.A., 2019. A comprehensive analysis of protocols for deriving dopaminergic neurons from human pluripotent stem cells. Stem Cells Transl. Med. 8 (4), 366–374. https://doi.org/10.1002/SCTM.18-0088.

Moher, D., Shamseer, L., Clarke, M., Ghersi, D., Liberati, A., Petticrew, M., Shekelle, P., Stewart, L.A., Estarli, M., Barrera, E.S.A., Martínez-Rodríguez, R., Baladia, E., Agüero, S.D., Camacho, S., Buhring, K., Herrero-López, A., Gil-González, D.M., Altman, D.G., Booth, A., et al., 2015. Preferred reporting items for systematic review and meta-analysis protocols (PRISMA-P) 2015 statement. Syst. Rev. 4 (1), 1. https://doi.org/10.1186/2046-4053-4-1, 2015 4:1.

Monzel, A.S., Smits, L.M., Hemmer, K., Hachi, S., Moreno, E.L., van Wuellen, T., Jarazo, J., Walter, J., Brüggemann, I., Boussaad, I., Berger, E., Fleming, R.M.T., Bolognin, S., Schwamborn, J.C., 2017. Derivation of human midbrain-specific organoids from neuroepithelial stem cells. Stem Cell Rep. 8 (5), 1144–1154. https://doi.org/10.1016/j.stemcr.2017.03.010.

Nickels, S.L., Modamio, J., Mendes-Pinheiro, B., Monzel, A.S., Betsou, F., Schwamborn, J. C., 2020. Reproducible generation of human midbrain organoids for in vitro modeling of Parkinson's disease. Stem Cell Res. 46. https://doi.org/10.1016/j.scr.2020.101870.

Nolbrant, S., Heuer, A., Parmar, M., Kirkeby, A., 2017. Generation of high-purity human ventral midbrain dopaminergic progenitors for in vitro maturation and intracerebral transplantation. Nat. Protoc. 12 (9), 1962–1979. https://doi.org/10.1038/NPROT.2017.078.

Palladino, V.S., Chiocchetti, A.G., Frank, L., Haslinger, D., McNeill, R., Radtke, F., Till, A., Haupt, S., Brüstle, O., Günther, K., Edenhofer, F., Hoffmann, P., Reif, A., Kittel-Schneider, S., 2020. Energy metabolism disturbances in cell models of PARK2 CNV carriers with ADHD. J. Clin. Med. 9 (12). https://doi.org/10.3390/JCM9124092.

Pamies, D., Wiersma, D., Katt, M.E., Zhao, L., Burtscher, J., Harris, G., Smirnova, L., Searson, P.C., Hartung, T., Hogberg, H.T., 2022. Human organotypic brain model as a tool to study chemical-induced dopaminergic neuronal toxicity. Neurobiol. Dis. 169. https://doi.org/10.1016/j.nbd.2022.105719.

Park, I.H., Arora, N., Huo, H., Maherali, N., Ahfeldt, T., Shimamura, A., Lensch, M.W., Cowan, C., Hochedlinger, K., Daley, G.Q., 2008. Disease-specific induced pluripotent stem cells. Cell 134 (5), 877–886. https://doi.org/10.1016/j.cell.2008.07.041.

Park, J.S., Davis, R.L., Sue, C.M., 2018. Mitochondrial dysfunction in parkinson's disease: new mechanistic insights and therapeutic perspectives. Curr. Neurol. Neurosci. Rep. 18 (5). https://doi.org/10.1007/S11910-018-0829-3.

Peng, J., Liu, Q., Rao, M.S., Zeng, X., 2013. Using human pluripotent stem cell-derived dopaminergic neurons to evaluate candidate Parkinson's disease therapeutic agents

in MPP+ and rotenone models. J. Biomol. Screen 18 (5), 522–533. https://doi.org/10.1177/1087057112474468.
Perrier, A.L., Tabar, V., Barberi, T., Rubio, M.E., Bruses, J., Topf, N., Harrison, N.L., Studer, L., 2004. Derivation of midbrain dopamine neurons from human embryonic stem cells. www.pnas.orgcgidoi10.1073pnas.0404700101.
Pintacuda, G., Martín, J.M., Eggan, K.C., 2021. Mind the translational gap: using iPS cell models to bridge from genetic discoveries to perturbed pathways and therapeutic targets. Mol. Autism 12 (1), 10. https://doi.org/10.1186/S13229-021-00417-X.
Pragmatic Review - York Health Economics Consortium. (n.d.). Retrieved January 23, 2026, from https://www.yhec.co.uk/glossary-term/pragmatic-review/.
Qian, X., Nguyen, H.N., Song, M.M., Hadiono, C., Ogden, S.C., Hammack, C., Yao, B., Hamersky, G.R., Jacob, F., Zhong, C., Yoon, K.J., Jeang, W., Lin, L., Li, Y., Thakor, J., Berg, D.A., Zhang, C., Kang, E., Chickering, M., et al., 2016. Brain-region-specific organoids using mini-bioreactors for modeling ZIKV exposure. Cell 165 (5), 1238–1254. https://doi.org/10.1016/j.cell.2016.04.032.
Quadrato, G., Brown, J., Arlotta, P., 2016. The promises and challenges of human brain organoids as models of neuropsychiatric disease. Nat. Med. 22 (11), 1220–1228. https://doi.org/10.1038/NM.4214.
Renner, H., Schöler, H.R., Bruder, J.M., 2021. Combining automated organoid workflows with artificial intelligence-based analyses: opportunities to build a new generation of interdisciplinary high-throughput screens for parkinson's disease and beyond. Mov. Disord. : Official Journal of the Movement Disorder Society 36 (12), 2745–2762. https://doi.org/10.1002/MDS.28775.
Reumann, D., Krauditsch, C., Novatchkova, M., Sozzi, E., Wong, S.N., Zabolocki, M., Priouret, M., Doleschall, B., Ritzau-Reid, K.I., Piber, M., Morassut, I., Fieseler, C., Fiorenzano, A., Stevens, M.M., Zimmer, M., Bardy, C., Parmar, M., Knoblich, J.A., 2023. In vitro modeling of the human dopaminergic system using spatially arranged ventral midbrain–striatum–cortex assembloids. Nat. Methods 20 (12), 2034–2047. https://doi.org/10.1038/S41592-023-02080-X;SUBJMETA.
Rifes, P., Kajtez, J., Christiansen, J.R., Schörling, A., Rathore, G.S., Wolf, D.A., Heuer, A., Kirkeby, A., 2024. Forced LMX1A expression induces dorsal neural fates and disrupts patterning of human embryonic stem cells into ventral midbrain dopaminergic neurons. Stem Cell Rep. 19 (6), 830–838. https://doi.org/10.1016/j.stemcr.2024.04.010.
Robicsek, O., Karry, R., Petit, I., Salman-Kesner, N., Müller, F.J., Klein, E., Aberdam, D., Ben-Shachar, D., 2013. Abnormal neuronal differentiation and mitochondrial dysfunction in hair follicle-derived induced pluripotent stem cells of schizophrenia patients. Mol. Psychiatr. 18 (10), 1067–1076. https://doi.org/10.1038/MP.2013.67.
Rossetti, A.C., Koch, P., Ladewig, J., 2019. Drug discovery in psychopharmacology: from 2D models to cerebral organoids. Dialogues Clin. Neurosci. 21 (2), 203–210. https://doi.org/10.31887/DCNS.2019.21.2/JLADEWIG.
Sabate-Soler, S., Nickels, S.L., Saraiva, C., Berger, E., Dubonyte, U., Barmpa, K., Lan, Y.J., Kouno, T., Jarazo, J., Robertson, G., Sharif, J., Koseki, H., Thome, C., Shin, J.W., Cowley, S.A., Schwamborn, J.C., 2022. Microglia integration into human midbrain organoids leads to increased neuronal maturation and functionality. Glia 70 (7), 1267–1288. https://doi.org/10.1002/GLIA.24167.
Sánchez-Danés, A., Consiglio, A., Richaud, Y., Rodríguez-Pizà, I., Dehay, B., Edel, M., Bové, J., Memo, M., Vila, M., Raya, A., Izpisua Belmonte, J.C., 2012. Efficient generation of A9 midbrain dopaminergic neurons by lentiviral delivery of LMX1A in human embryonic stem cells and induced pluripotent stem cells. Hum. Gene Ther. 23 (1), 56–69. https://doi.org/10.1089/HUM.2011.054.
Sarrafha, L., Parfitt, G.M., Reyes, R., Goldman, C., Coccia, E., Kareva, T., Ahfeldt, T., 2021. High-throughput generation of midbrain dopaminergic neuron organoids from reporter human pluripotent stem cells. STAR Protoc. 2 (2). https://doi.org/10.1016/j.xpro.2021.100463.
Sheng, Y., Filichia, E., Shick, E., Preston, K.L., Phillips, K.A., Cooperman, L., Lin, Z., Tesar, P., Hoffer, B., Luo, Y., 2016. Using iPSC-derived human DA neurons from opioid-dependent subjects to study dopamine dynamics. Brain and Behavior 6 (8). https://doi.org/10.1002/BRB3.491.
Slanzi, A., Iannoto, G., Rossi, B., Zenaro, E., Constantin, G., 2020. In vitro models of neurodegenerative diseases. Front. Cell Dev. Biol. 8. https://doi.org/10.3389/FCELL.2020.00328.
Smits, L.M., Reinhardt, L., Reinhardt, P., Glatza, M., Monzel, A.S., Stanslowsky, N., Rosato-Siri, M.D., Zanon, A., Antony, P.M., Bellmann, J., Nicklas, S.M., Hemmer, K., Qing, X., Berger, E., Kalmbach, N., Ehrlich, M., Bolognin, S., Hicks, A.A., Wegner, F., et al., 2019. Modeling Parkinson's disease in midbrain-like organoids. npj Parkinson's Dis. 5 (1). https://doi.org/10.1038/s41531-019-0078-4.
Soliman, M.A., Aboharb, F., Zeltner, N., Studer, L., 2017. Pluripotent stem cells in neuropsychiatric disorders. Mol. Psychiatr. 22 (9), 1241–1249. https://doi.org/10.1038/MP.2017.40.
Sonntag, K.-C., Pruszak, J., Yoshizaki, T., van Arensbergen, J., Sanchez-Pernaute, R., Isacson, O., 2007. Enhanced yield of neuroepithelial precursors and midbrain-like dopaminergic neurons from human embryonic stem cells using the bone morphogenic protein antagonist noggin. Stem Cell. 25 (2), 411–418. https://doi.org/10.1634/stemcells.2006-0380.
Sozzi, E., Nilsson, F., Kajtez, J., Parmar, M., Fiorenzano, A., 2022. Generation of human ventral midbrain organoids derived from pluripotent stem cells. Curr. Protoc. 2 (9). https://doi.org/10.1002/cpz1.555.
Sundberg, M., Bogetofte, H., Lawson, T., Jansson, J., Smith, G., Astradsson, A., Moore, M., Osborn, T., Cooper, O., Spealman, R., Hallett, P., Isacson, O., 2013. Improved cell therapy protocols for Parkinson's disease based on differentiation efficiency and safety of hESC-, hiPSC-, and non-human primate iPSC-derived dopaminergic neurons. Stem Cells (Dayton, Ohio) 31 (8), 1548–1562. https://doi.org/10.1002/STEM.1415.
Swistowski, A., Peng, J., Liu, Q., Mali, P., Rao, M.S., Cheng, L., Zeng, X., 2010. Efficient generation of functional dopaminergic neurons from human induced pluripotent stem cells under defined conditions. Stem Cell. 28 (10), 1893–1904. https://doi.org/10.1002/stem.499.
Tabata, Y., Imaizumi, Y., Sugawara, M., Andoh-Noda, T., Banno, S., Chai, M.C., Sone, T., Yamazaki, K., Ito, M., Tsukahara, K., Saya, H., Hattori, N., Kohyama, J., Okano, H., 2018. T-type calcium channels determine the vulnerability of dopaminergic neurons to mitochondrial stress in familial parkinson disease. Stem Cell Rep. 11 (5), 1171. https://doi.org/10.1016/J.STEMCR.2018.09.006.
Takahashi, K., Tanabe, K., Ohnuki, M., Narita, M., Ichisaka, T., Tomoda, K., Yamanaka, S., 2007. Induction of pluripotent stem cells from adult human fibroblasts by defined factors. Cell 131 (5), 861–872. https://doi.org/10.1016/j.cell.2007.11.019.
Takahashi, K., Yamanaka, S., 2006. Induction of pluripotent stem cells from mouse embryonic and adult fibroblast cultures by defined factors. Cell 126 (4), 663–676. https://doi.org/10.1016/j.cell.2006.07.024.
Tesco, G., Lomoio, S., 2022. Pathophysiology of neurodegenerative diseases: an interplay among axonal transport failure, oxidative stress, and inflammation? Semin. Immunol. 59. https://doi.org/10.1016/j.smim.2022.101628.
Tieng, V., Stoppini, L., Villy, S., Fathi, M., Dubois-Dauphin, M., Krause, K.H., 2014. Engineering of midbrain organoids containing long-lived dopaminergic neurons. Stem Cell. Dev. 23 (13), 1535–1547. https://doi.org/10.1089/scd.2013.0442.
Van Inzen, W.G., Peppelenbosch, M.P., Van Den Brand, M.W.M., Tertoolen, L.G.J., De Laat, S.W., 1996. Neuronal differentiation of embryonic stem cells. Biochim. Biophys. Acta Mol. Cell Res. 1312 (1), 21–26. https://doi.org/10.1016/0167-4889(96)00011-0.
Volpicelli, F., Perrone-Capano, C., Bellenchi, G.C., Colucci-D'Amato, L., Di Porzio, U., 2020. Molecular regulation in dopaminergic neuron development. Cues to unveil molecular pathogenesis and pharmacological targets of neurodegeneration. Int. J. Mol. Sci. 21 (11), 1–19. https://doi.org/10.3390/IJMS21113995.
Wang, R.C., Wang, Z., 2023. Precision medicine: disease subtyping and tailored treatment. Cancers 15 (15). https://doi.org/10.3390/CANCERS15153837.
Xi, J., Liu, Y., Liu, H., Chen, H., Emborg, M.E., Zhang, S.C., 2012. Specification of midbrain dopamine neurons from primate pluripotent stem cells. Stem Cells (Dayton, Ohio) 30 (8), 1655–1663. https://doi.org/10.1002/STEM.1152.
Xia, N., Zhang, P., Fang, F., Wang, Z., Rothstein, M., Angulo, B., Chiang, R., Taylor, J., Reijo Pera, R.A., 2016. Transcriptional comparison of human induced and primary midbrain dopaminergic neurons. Sci. Rep. 6. https://doi.org/10.1038/SREP20270.
Xu, H., Yang, F., 2022. The interplay of dopamine metabolism abnormalities and mitochondrial defects in the pathogenesis of schizophrenia. Transl. Psychiatry 12 (1). https://doi.org/10.1038/S41398-022-02233-0.
Yamaguchi, A., Ishikawa, K. ichi, Inoshita, T., Shiba-Fukushima, K., Saiki, S., Hatano, T., Mori, A., Oji, Y., Okuzumi, A., Li, Y., Funayama, M., Imai, Y., Hattori, N., Akamatsu, W., 2020. Identifying therapeutic agents for amelioration of mitochondrial clearance disorder in neurons of familial parkinson disease. Stem Cell Rep. 14 (6), 1060–1075. https://doi.org/10.1016/j.stemcr.2020.04.011.
Yde Ohki, C.M., Walter, N.M., Bender, A., Rickli, M., Ruhstaller, S., Walitza, S., Grünblatt, E., 2023. Growth rates of human induced pluripotent stem cells and neural stem cells from attention-deficit hyperactivity disorder patients: a preliminary study. JNT (J. Neural Transm.) 130 (3), 243–252. https://doi.org/10.1007/S00702-023-02600-1.
Zeng, X., Chen, J., Deng, X., Liu, Y., Rao, M.S., Cadet, J.L., Freed, W.J., 2006. An in vitro model of human dopaminergic neurons derived from embryonic stem cells: MPP+ toxicity and GDNF neuroprotection. Neuropsychopharmacology: Official Publication of the American College of Neuropsychopharmacology 31 (12), 2708–2715. https://doi.org/10.1038/SJ.NPP.1301125.